

## **Chapter- 5**

# **The molecular mechanism of *in vitro* and *in vivo* anticancer potential of biogenic AuNPI3Cs against Ehrlich ascites carcinoma (EAC) cells**

### **5.1 Introduction**

### **5.2 Materials and methods**

### **5.3 Results**

### **5.4 Discussion**

### **5.5 Conclusion**

## Abstract

Green synthesis of gold nanoparticles has attained much attention as a simple and environment-friendly alternative to conventional chemical synthesis. This study was designed to investigate the antiproliferative and apoptotic activity of biogenic gold nanoparticles (AuNPI3Cs) against Ehrlich ascites carcinoma (EAC) cells *in vitro* and *in vivo*. MTT assay, ROS measurement, acridine orange and ethidium bromide double staining, PI and DAPI staining, cell cycle study and Annexin V analyses by flow cytometry were done to explore the mode of AuNPI3Cs induced cell death. DNA laddering, measurement of generation of reactive oxygen species using H<sub>2</sub>DCFDA stain, mitochondrial membrane potential by rhodamine 123, JC-1 stain and Western blot analysis were performed to explore the pathways involved in the apoptosis. Antitumor activities of AuNPI3Cs were investigated in EAC bearing mice and EAC-induced solid tumour model at the dose level of 1.5 mg/kg body wt. In EAC bearing mice haematological parameters, change in body weight, tumour volume, viable tumour cell count, mean survival time, oxidative stress parameters and anti-angiogenic activity were investigated after consecutive 14 days treatment of AuNPI3Cs at 1.5 and 3mg/kg body wt in case of EAC cell. MTT results showed that AuNPI3Cs inhibited the growth of EAC cells, with IC<sub>50</sub> values of 5 µg ml<sup>-1</sup>. Membrane blebbing of AuNPI3Cs treated cells was observed under polarizing light microscopic. PI and DAPI staining showed condensed chromatin in AuNPI3Cs treated cells. Cell cycle arrest at G<sub>2</sub>/M phase were observed in EAC cells. AO-EtBr double staining and Annexin V-FITC and PI staining revealed that AuNPI3Cs induced cell death occurred via apoptosis not necrosis. Further investigation into the DNA fragmentation and alteration of mitochondrial membrane potential and generation of reactive oxygen species (ROS) revealed that AuNPI3Cs treatment induced apoptosis in EAC cells via up-regulation of Bax, caspase-3 and down-regulation of Bcl-2 proteins which noted in Western blot analysis. In AuNPI3Cs treated group, tumour volume

and viable tumour cell count became decreased. Altered haematological and antioxidant parameters were restored significantly towards normal level. Moreover the mean survival time of treated mice was elevated significantly compared to untreated control group animals. Immunohistochemical study showed that Ki67 and CD-31 expression were inhibited significantly in AuNPI3Cs and 5-FU treated solid tumors. It can be concluded that AuNPI3Cs induced an anti-proliferative effect that led to cell cycle arrest and apoptosis through mitochondria-mediated intrinsic pathway.

## **5.1 Introduction**

Cancer is a principal leading disease contributor in humans worldwide. Even though a huge effort and the progress were done to fight cancer either in preclinical research or in clinical advances, many limitations still presented and needed to be improved. Cancer is a major cause of mortality and in spite of unexpected effort over the past several decades, successful abolition and control remains imperceptible (Jemal et al., 2008). Cancer is considered as a heterogeneous collection of cells that advance in tumour microenvironments (Aktipis et al., 2013).

### **5.1.4. Ehrlich ascites carcinoma (EAC)**

Ehrlich ascites carcinoma is a spontaneous murine mammary adenocarcinoma (Ehrlich and Apolant, 1905) adapted to ascites form. Ehrlich ascites carcinoma (EAC) which is a cancer cell line model, is the most well-known ascites carcinoma. It has been reported that Ehrlich ascites tumor cells are the reason for their rapid proliferation in almost any mouse host (Patt and Straube, 1956). EAC is undifferentiated carcinoma that is initially hyperdiploid. It has transplanted ability potential, shorter life span, rapid proliferation, very enormous malignancy (Kaleoğlu and İşli, 1977). It has a transplantable capacity for certain quantitative tumour cells to another host mouse (Klein, 1951).

### **5.1.5 Angiogenesis**

Angiogenesis, the formation of new blood vessels helps the growth of both solid and ascites tumour (Perez-Atayde et al., 1997). Solid tumour start to develop as immature avascular nodule and vascularization could grow and can enhance tumour progression. The tumour cells get oxygen and nutrients from neovascularization. Entry of tumour cell into the circulation is enhanced by the undeveloped neo-vessels and thus metastasis develops (Liotta and Stracke, 1988). For tumor development angiogenesis is an essential condition. The dimensions of a tumour cannot exceed 2-3 mm<sup>3</sup> without proper blood supply (Folkman, 1995). Pro-angiogenic and anti-angiogenic molecules control the balance of angiogenesis (Hanahan and Weinber, 2000).

### **5.1.6 Oxidative stress and antioxidant defence**

Free radicals such as superoxide anion, hydroxyl radicals and non-radical species such as hydrogen peroxide, singlet oxygen are different forms of reactive oxygen species (ROS) that generates oxidative stress (Finkel et al., 2000). Balance in the production of free radicals may protect the healthy tissue from oxidative stress by the help of active antioxidants (Tiwari, 2001). Oxidative damage created by free radical generation is a critical etiological factor that implicated in several chronic human diseases such as diabetes mellitus, cancer, atherosclerosis, arthritis and neurodegenerative diseases and also in the aging process. Antioxidant therapy has gained an enormous significance in treatment of these diseases (Mate's et al., 1999).

### **5.1.7 Ehrlich ascites carcinoma and role of medicinal plant**

Several medicinal plants were reported to stimulate the immune system in different pathways. *Securidaca longepedunculata* caused a decrease in angiogenesis as reduced body weight of

treated animals and a reduction in volume of ascitic fluid in treated mice. DNA fragmentation assay of Ehrlich ascites carcinoma cells from treated animals depicted a possible proapoptotic effect of *S. longepedunculata* extract due to the ladder forming pattern. The expression of proapoptotic proteins and cell cycle arrest protein p53 in cytoplasm in the nuclei of Ulvan polysaccharide treated EAC cells were remarkably increased while the anti-apoptotic protein Bcl-2 expression was decreased (Lawal et al., 2012).

Methanol extract of *Eucalyptus camaldulensis* treated EAC cells showed membrane blebbing, chromatin condensation, and nuclear fragmentation in Hoechst 33342 staining. The DNA profile in agarose gel electrophoresis also confirmed that EAC cell death by extract through the apoptosis (Islam et al., 2014).

#### **5.1.6. Gold nanoparticles on Ehrlich ascites tumor**

Some researchers reported regarding the effect of gold nanoparticles on transplantable ascites tumour. Medhat et al., 2017 reported that dextran-capped gold nanoparticles provide significant antitumor effects in both Ehrlich ascites and solid tumor in mice models.

Galactoxyloglucan polysaccharide coated gold nanoparticles are more potent in inhibiting the proliferation and tumor growth of murine cancer cells *in vitro* and *in vivo* against Ehrlich ascites cell. (Joseph et al., 2013).

The aim of this chapter is to study the anti-proliferative as well as apoptotic activity of AuNPI3Cs via mitochondrial pathway and production of ROS against EAC cells in *in-vitro* and *in-vivo* condition.

## **5.2 Materials and methods**

### **5.2.1 Chemicals and culture media**

EDTA, Tris buffer, titron X-100, phenol, chloroform, iso-amyl alcohol, ethidium bromide (EtBr), 5,5'-Dithio-bis-(2-nitrobenzoic Acid) (DTNB) and 2-vinylpyridine were purchased from Merck Millipore (India) Pvt. Ltd., Mumbai. All other chemicals were from Merck Ltd., SRL Pvt. Ltd., Mumbai, Himedia India, Ltd., Mumbai, India.

### **5.2.2 Animal maintenance**

Swiss albino mice, 8-10 weeks old, weighing 18-24 g were used and fed with standard pellet diet and water *ad libitum* and under controlled conditions of temperature and humidity with 12 h light/dark cycle. EAC cells were maintained in Swiss albino mice at the concentration of  $1 \times 10^6$  cells /ml (Maiti Choudhury et al., 2010).

The study was approved by the Institutional Animal Ethical Committee, registered under Committee for the Purpose of Control and Supervision of Experiments on Animals (CPCSEA), Ministry of Environment, Forests & Climate Change, Govt. of India (approval No. IEC/7-14/C14-16).

### **5.2.3 Cancer cell culture**

Ehrlich ascites carcinoma (EAC) cells were obtained from Chittaranjan National Cancer Institute, Kolkata, India. Cells were grown in DMEM medium (GIBCO BRL, USA) containing 10% FBS and antibiotics in appropriate conditions. The cells were maintained by intraperitoneal inoculation ( $2 \times 10^6$  cells/mouse) in the above said mice. After washing, EAC cells free from contaminating RBC were cultured in RPMI-1640 medium supplemented with 10% foetal bovine serum (FBS) and antibiotic solution (100 U ml<sup>-1</sup> penicillin, 10 mg ml<sup>-1</sup> streptomycin and 4 mM L-glutamine) under 5% CO<sub>2</sub> and 95% humidified atmosphere at 37°C in a CO<sub>2</sub> incubator and used for different experiments.

#### **5.2.4 Isolation of mouse lymphocytes**

Isolation of mice lymphocytes was performed according to the modified method of Hudson and Hay, which was described in chapter-3.

#### **5.2.5 Experimental Design**

*In vitro* cytotoxicity of AuNPI3Cs was performed against EAC cells. EAC ( $1 \times 10^6$  cells ml<sup>-1</sup>) cells were treated with AuNPI3Cs at different concentrations (0.5, 1, 2, 5, 10, 25 µg/ml) for 24 h. After the treatment, the cells were collected from the culture plates. EAC cells were washed two times by 0.1 M PBS (pH 7.4) at 1200 rpm for 5 min at 4°C. Then washed EAC cells were used for the measurement of different oxidative stress and apoptosis biomarkers.

#### **5.2.6 *In vitro* cytotoxicity study by MTT assay**

The method was described previously in chapter 4. The effect of AuNPI3Cs on the proliferation of EAC cells were expressed as the % of cell viability using the following formula:

$$\% \text{ cell viability} = [\text{OD sample} - \text{OD control}] \times 100 / \text{OD control}$$

#### **5.2.7 *In vitro* drug uptake assay**

In order to explore the intracellular uptake of AuNPI3Cs, EAC cells ( $1 \times 10^6$  cells ml<sup>-1</sup>) were treated with 5 µg ml<sup>-1</sup> of rhodamine B (0.05%)-labelled AuNPI3Cs for 4-6 h under 5% CO<sub>2</sub> and 95% humidified atmosphere at 37°C in a CO<sub>2</sub> incubator. The cellular distributions of rhodamine B-labeled AuNPI3Cs were observed by fluorescence microscopy (Nikon Eclipse LV100POL). Images were captured at 40x optical zoom and analysis was done using Image J software v. r. 1.43 (NIH).

Drug uptake study in EAC cells was also performed by atomic absorption spectroscopy (AAS) and 6th hour treatment was selected for AAS study. After the treatment, cells were twice PBS buffer washed and re-suspended in 6 M nitric acid and incubated at 95°C for 24 h. The drug content were then assayed (Gliga et al., 2014) with atomic absorption spectrophotometer (Shimadzu AA-7000).

#### **5.2.8 Estimation of reduced glutathione (GSH)**

The procedure is same as it is described in chapter 4 (Griffith 1981).

#### **5.2.9 Determination of oxidized glutathione (GSSG)**

The oxidized glutathione level was performed according to the modified method of Griffith, 1980 was previously described in chapter 4.

#### **5.2.10 Intracellular ROS measurement**

Intracellular ROS measurement (Roy et al.,2008) was previously described in chapter 4.

#### **5.2.11 Cellular morphology study by polarizing microscopy and scanning electron microscopy**

EAC cells ( $1 \times 10^6$  cells  $\text{ml}^{-1}$ ) were treated with AuNPI3Cs at  $\text{IC}_{50}$  dose in DMEM media supplemented with 10% FBS, 95% humidified atmosphere and incubated at 37°C with 5%  $\text{CO}_2$  for 24 h. After incubation, membrane blebbing of EAC cells were examined under polarizing microscope (NIKON ECLIPSE LV100POL, Germany) and image of each field was captured (Venkatesan et al.,2011).

After treatment, EAC cells were washed with PBS and fixated with 2.5% glutaraldehyde in 0.1 M phosphate buffer (pH 7.4) for 1h at room temperature. Then dehydration process was accomplished by in 50%, 70%, 90% ethanol and 100% ethanol. Then subjected on cover slip and dried in vacuum desiccator and mounted on stub. Subsequently, the dried samples were examined (Tang et al., 2014) with a scanning electron microscope (Carl Zeiss, Germany, EVO18).

### **5.2.12 Lactate dehydrogenase release assay**

EAC cells ( $1 \times 10^6$  cells  $\text{ml}^{-1}$ ) were treated with AuNPI3Cs at  $\text{IC}_{50}$  dose in a 96-well plate for LDH release assay (Al-Qubaisiet al.2011) and then incubated for 24 h. After that 40  $\mu\text{l}$  of media was taken from each well and 6% triton X-100, 4.6 mM pyruvic acid in PBS buffer (pH 7.5) were mixed to it followed by addition of 100  $\mu\text{l}$  of 0.4  $\text{mg ml}^{-1}$  reduced NADH in 0.1 M PBS buffer (pH 7.5). Then the absorbance was noted at 340 nm for 1 min in an ELISA microplate reader (Bio-Rad, Model 680).

### **5.2.13 Chromatin condensation by PI and DAPI staining**

The method was previously described in chapter 4.

### **5.2.14 Acridine orange–ethidium bromide double staining**

EAC cells ( $1 \times 10^6$  cells  $\text{ml}^{-1}$ ) were seeded into each well and  $\text{IC}_{50}$  doses of AuNPI3Cs were added to the each well of plate and incubated at  $37^\circ\text{C}$  in a humidified 5%  $\text{CO}_2$  atmosphere for 24 h. After washing with PBS buffer, 10  $\mu\text{l}$  of cells were mixed with 10  $\mu\text{l}$  each of acridine orange ( $50 \mu\text{g ml}^{-1}$ ) and ethidium bromide ( $50 \mu\text{g ml}^{-1}$ ) (Ho et al., 2009). Then the cells were placed on a clean glass slide and observed under a fluorescence microscope (LEICA DFC295, Germany).

### **5.2.15 TUNEL assay**

Apoptosis was also examined by using the Terminal deoxynucleotidyl transferase-mediated dUTP nick end labeling (TUNEL) assay to detect DNA strand breaks during apoptosis using an In Situ Cell Death Detection Kit, fluorescein, version: 17 (cat no: 11684795910) according to the manufacturer's instructions (Sgonc et al., 1994). Briefly, EAC cells were treated with AuNPI3Cs ( $5 \mu\text{g ml}^{-1}$ ) for 24 h and fixed with freshly prepared 3.7% paraformaldehyde in

phosphate-buffered saline (PBS; pH 7.4) for 30 min. The EAC cells were then suspended with 100 ml permeabilization solution (0.1% Triton X-100 in 0.1% sodium citrate buffer) for 2 min in ice-chilled condition. The suspended cells were washed three times with PBS buffer and incubated with 50 ml TUNEL reaction mixture for 60 min at 37°C. The stained cells were analysed using flow cytometer (BD FACSVerse) an excitation wavelength in the range of 488 nm and detection in the range of 515.565 nm.

#### **5.2.16 Genotoxicity study by alkaline comet assay**

The procedure is described in chapter 3 (Alcantra et al., 2011).

#### **5.2.17 Measurement of Mitochondrial membrane potential ( $\Delta\Psi_m$ )**

The method is previously described in chapter 4 (M'memba et al., 2006).

#### **5.2.18 Detection of apoptosis by Annexin V-FITC apoptosis detection kit**

Detection of apoptosis was performed using Annexin V-FITC Apoptosis Detection Kit (Abgenex, Cat: 1001K). Briefly, EAC cells ( $1 \times 10^6$  cells ml<sup>-1</sup>) were plated and treated with AuNPI3Cs at IC<sub>50</sub> dose of (5µg/ml) for 24 h. After that, the cells were washed with phosphate buffer saline (pH 7.4), resuspended in 1x Annexin V binding buffer, and stained with Annexin V-FITC and PI in the dark for 15 min at room temperature. Apoptotic cells were detected using flow cytometer (BD FACS Verse) and Cell Quest software.

#### **5.2.19 Analysis of cell cycle disruption by flow cytometry**

The method of cell cycle analysis by flow cytometry (Evans et al.,2000) was described in chapter 4.

#### **5.2.20 Western blot analysis:**

Western blot analysis was done according to the previously described in chapter 4.

#### **5.2.21 *In vivo* study**

Forty eight Swiss albino male mice were divided into four groups having twelve in each group except Group I which contained six mice.  $1 \times 10^6$  EAC cells/mouse were given intraperitoneally to animals of all groups except Group I (Saline control) and this was designated as day zero. Group II (EAC control) was considered as tumour control group. After 24 h of tumour inoculation AuNPI3Cs in two doses were injected intraperitoneally to group III (AuNPI3Cs-1.5mg/kg body weight) and IV( AuNPI3Cs -3mg/kg body weight) and group V (5-FU-20 mg/kg body weight) received standard drug 5-FU once daily for 14 consecutive days (Haldar et al., 2010). From the day of zero to the last day animal body weight change were recorded daily (Maiti et al., 2010). For the estimation of haematological parameters, blood was collected from each mice. Ascites fluid was drawn from peritoneal cavity of each mice for the study of tumour regression parameters (Gupta et al., 2004). Liver and kidney tissues were collected for the study of hepatic and renal oxidative stress parameters. The remaining alive 6 mice of Group III - V each were checked on a daily basis to record the mean survival time.

### **5.2.22 Change in Body weight**

Thirty male mice were taken to observe body weight change and divided into five groups (n=6). Tumour growth was observed in terms of daily body weight change and recorded from the day of zero to the last day (Maiti et al.,2010).

### **5.2.23 Studies on host survival time and increase life span**

The mean survival time (MST) and Increase life span (ILS) were calculated (Jacob and Latha, 2013) by the following equations.

Mean survival time = (Day of 1st death + Day of last death)/2,

Increase life span (ILS) (%) = [(Mean survival time of treated group/mean survival time of control group) - 1] x 100

#### **5.2.24 Tumour volume**

At the time of sacrifice, injected normal saline were aspirated from the peritoneal cavity of mice aseptically. The tumour volume was calculated by the following way:

Tumour volume = Volume of saline and tumour cells (ml) – Volume of saline (ml).

Then each of the calculated tumour volume is compared with tumour control group (Bala et al., 2010).

#### **5.2.25 Tumour cell count**

The ascitic fluid was taken aseptically from peritoneal cavity of each mouse and diluted 100 times with phosphate buffer saline. Then a drop of the diluted cell suspension was charged in Neubauer counting chamber and the numbers of tumour cells were counted in the 64 small squares (Saha et al., 2011).

#### **5.2.26 Haematological analysis**

##### **5.2.26.1 Red blood cell (RBC) count (Wintrobe, 1967)**

The method of red blood cell count has been described in chapter 3.

##### **5.2.26.2 White blood cell (WBC) count (Wintrobe, 1967)**

The method of white blood cell count has been described in chapter 3.

##### **5.2.26.3 Determination of haemoglobin (Dacie and Lewis, 1975)**

The haemoglobin percentage was determined by cyanmethaemoglobin method and the method has been described in chapter 3.

## **5.2.27 Antioxidant Parameters**

### **5.2.27.1 Estimation of malondialdehyde (MDA) content**

Firstly, one ml of liver and kidney homogenate (20 mg/ml phosphate buffer) was mixed with 0.2 ml of 8.1% sodium dodecyl sulfate, 1.5 ml of acetate buffer (20% pH 3.5) and 1.5 ml of aqueous solution of thiobarbituric acid (0.8%). After heating of that mixture at 95°C for 60 min red pigment was formed. After that 5 ml of *n*-butanol-pyridine mixture (15: 1) was used for its extraction and centrifuged at 5000 rpm at room temperature for 10 min. The optical density was noted at 535 nm (Ohkawa et al., 1979).

### **5.2.27.2 Estimation of reduced glutathione (GSH)**

At first, 200 µl of liver and kidney homogenate was mixed with 100 µl sulfosalicylic acid and the mixture was centrifuged at 3000 rpm for 10 min. Then 1.8 ml of DTNB was mixed with 200 µl of supernatant. The supernatant was shaken well and the optical density was noted at 412 nm (Griffith, 1981).

### **5.2.27.3 Estimation of superoxide dismutase (SOD)**

For the estimation of superoxide dismutase (SOD) of liver and kidney homogenate, 10 µl of homogenate, 100 µl of 2 mM pyrogallol and 2 ml of buffer mixture (50 mM TrisHCl, 10 mM hydrochloric acid (HCl) and 1 mM EDTA) were poured in glass cuvette and the absorbance was measured at 420 nm for 3 min.

### **5.2.27.4 Estimation of catalase (CAT)**

Estimation of catalase was performed by the method of Aebi, 1974. After mixing of 1 ml of 30mM H<sub>2</sub>O<sub>2</sub> and 1.9ml of 15mM PBS in 0.1ml of homogenate, readings were taken in the spectrophotometer at 30 sec interval at 240nm.

#### **5.2.27.5 Estimation of glutathione peroxidase (GPx)**

At first, homogenates (0.2 ml) were mixed with 0.1 ml of 2.5 mM H<sub>2</sub>O<sub>2</sub>, 0.2 ml of 0.4 M sodium phosphate buffer, 0.1 ml of 10 mM sodium azide and 0.2 ml of 4 mM reduced glutathione and was incubated for 5 min at 37°C. After that 0.4 ml of 10% TCA was added to that mixture to stop the reaction and centrifuged at 3200 rpm for 20 min. Then 3 ml of di sodium hydrogen phosphate (Na<sub>2</sub>HPO<sub>4</sub>) and 1 ml of 5, 5'-dithiobisnitrobenzoic acid (DTNB) were added to 0.5 ml of supernatant. The absorbance was measured at 420 nm (Rotruck et al., 1973).

#### **5.2.27.6 Estimation of glutathione-s-transferase (GST)**

Glutathione-S-transferase (GST) activity was determined by taking 0.1 ml of homogenate was mixed with 0.2 ml of 100 mM PBS, 0.05 ml of 1 mM GSH, 0.02 ml of 60mM 1-Chloro-2, 4 dinitrobenzene (CDNB) in a glass cuvette for measuring optical density at 340nm (Habig et al, 1974).

#### **5.2.28 Treatment in EAC induced solid tumour model**

At logarithmic growth phase EAC cells were collected and suspended in PBS at  $1 \times 10^6$  cells/0.1ml and then in the right flank of each mouse the cells were injected subcutaneously. When tumour volumes developed 90-100 mm<sup>3</sup> (after 10 days) the animals were randomly divided into three groups containing six animals in each group. Before the beginning of treatment, body weight and tumour volume of all tumour-bearing mice were recorded. Then for 28 days, AuNPI3Cs were injected subcutaneously in the following schedule: (i) EAC control; (ii) AuNPI3Cs (1.5 mg/kg/day); (iii) 5-FU (20 mg/kg/day).

On day 29<sup>th</sup>, at the end of the treatment period, the mice were sacrificed by cervical dislocation. The tumours were removed from mice and with vernier callipers each tumor volume was measured and calculated using the formula:  $V=(L \times W^2) \pi/6(3)$ , where L (mm) is the longest diameter and W (mm) is perpendicular to L (Sarkar et al., 2010). After fixing the tumor in formalin it was embedded in paraffin for immunohistochemical analysis.

Percent inhibition of tumour =

$$\frac{\text{Average tumour volume of control} - \text{Average tumour volume of treated}}{\text{Average tumour volume of control}} \times 100 \quad (4)$$

### 5.2.29 Immunohistochemical (IHC) study

EAC cell proliferation and angiogenesis were performed using Ki-67, CD31 antibodies in EAC-induced mice tumours by immunohistochemical technique. Sections were fixed, deparaffinized, rehydrated in graded alcohols (100%, 95% and 80% v/v) and then washed in distilled water. With 0.05% trypsin and 0.05% CaCl<sub>2</sub> in Tris-HCl (pH 7.6), tissue sections were preserved for 5 min at 37°C. The sections were incubated for 30 min in 10 mM/L citric acid (pH 6.0). For antigen retrieval slides were then washed and blocked with 2% BSA in TBST for 30 min. Incubation of tissue sections with antiserum to Ki-67, CD31 (1:50) were done for 3 h at room temperature. After two times PBS washing, further incubation were done with secondary immunoglobulins (1:500) for 45 min at room temperature. Then the slides were labelled with avidin-biotin peroxidase complexes (1:25) for 30 min at room temperature after twice PBS washing. Lastly, the sections were counter-stained with Meyer's hematoxylin. Then proper dehydration with alcohol and cleanin by xylene and the tissue was mounted with DPX and observed using a polarizing microscope (NIKON ECLIPSE LV100POL) (Sarkar et al., 2010).

### **5.2. 30 Histopathological study**

For histopathological examinations, organs such as liver, kidney were collected from sacrificed animals of all the groups. The collected organs were weighed and dipped into 10% neutral buffered formalin for preservation. Then the tissues were dehydrated in graded alcohols and embedded in paraffin. Tissues were cut in five micron thickness and the sections were stained with haematoxylin and eosin (H and E) for histopathological study (Standish et al., 2006).

#### **5.2.31 Statistical analysis**

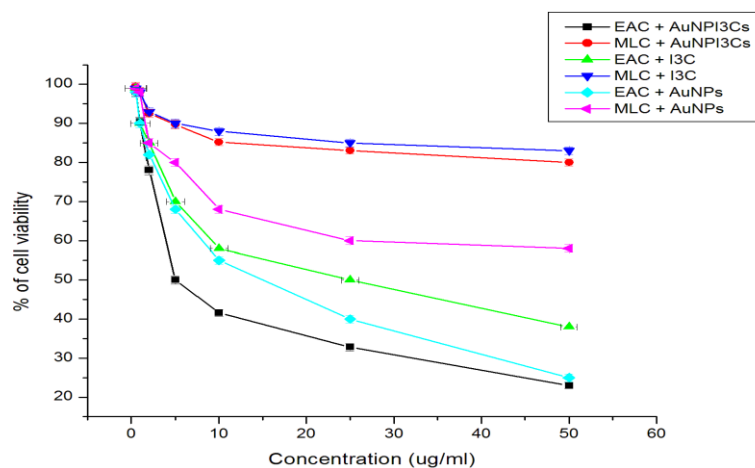
All the experiments were done in triplicate manner. The results were expressed as Mean  $\pm$  SEM. Comparisons between the means of the control and treated groups were calculated by using the one-way ANOVA test (using a statistical package, Origin 6.1, Northampton, MA),  $p < 0.05$  as a limit of significance.

### **5.3 Results**

#### **5.3.1 Effect of AuNPs and AuNPI3Cs on *in vitro* cytotoxicity against EAC cells.**

The dose-dependent *in vitro* cytotoxicity was detected (Figure 5.3 A) in AuNPI3Cs treated EAC cells. EAC cell viability was decreased significantly 3%, 9.69%, 15.86%, 49.75%, 58% and 68.78% by AuNPI3Cs at 0.5, 1, 2.5, 5, 10 and 25  $\mu\text{g ml}^{-1}$ . The viability of MLC was also not significantly altered up to 25  $\mu\text{g ml}^{-1}$  dose level of AuNPI3Cs (Figure 5.3A). At  $\text{IC}_{50}$  values (5  $\mu\text{g ml}^{-1}$ ) of AuNPI3Cs for EAC cells, no *in vitro* cytotoxicity was detected in mouse lymphocytes. So, our further experiments on EAC cells were carried out using these respective  $\text{IC}_{50}$  concentrations. But after treatment of chemically synthesized AuNPs, cell viability of mice lymphocytes were reduced significantly as well as cancer cells.

Figure 5.3. Effect of AuNPI3Cs on *in vitro* cytotoxicity against EAC cells and MLCs. Cells were treated with AuNPI3Cs for 24 h at 37°C. Values are expressed as Mean±SEM of three experiments.



### 5.3.2 Intracellular uptake of AuNPI3Cs in EAC cells

The fluorescence imaging detected that cellular internalization of rhodamine labeled AuNPI3Cs was observed in EAC cells (Figure 5.4) throughout the cytoplasm, indicating the effective uptake of AuNPI3Cs in EAC cells. Drug uptake was also assessed by AAS and it was shown that Au<sup>+</sup> ion uptake was significantly elevated in EAC cells at 5 µg ml<sup>-1</sup> dose for 2, 4 and 6 h (Figure 5.4B).

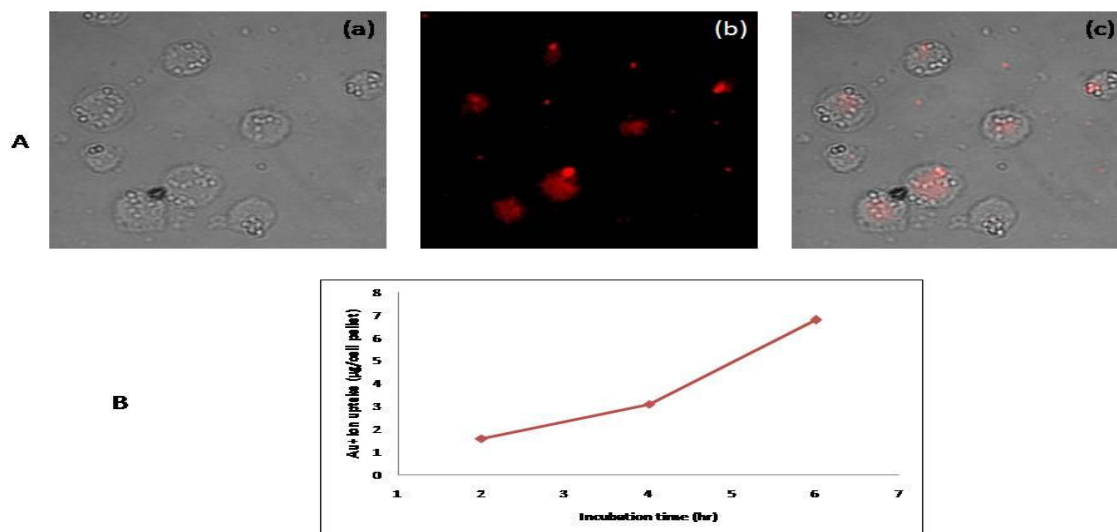


Figure 5.4.A Fluorescence image of intracellular uptake of AuNPI3Cs in EAC cell. B Estimation of intracellular uptake of Au<sup>+</sup> ion in EAC cell by atomic absorption spectroscopy.

### 5.3.3 Effect of AuNPI3Cs on GSH and GSSG content of EAC cells

The present study revealed that the levels of GSH in EAC cells by 5-FU and AuNPI3Cs (Figure 5.5A). AuNPI3Cs significantly ( $p < 0.001$ ) diminished the GSH level EAC cells at IC<sub>50</sub> dose. The level of GSSG was increased in AuNPI3Cs and 5-FU treated EAC cells at IC<sub>50</sub> dose (Figure 5.5B). After AuNPI3Cs treatment, the GSSG level was significantly ( $p < 0.001$ ) increased in EAC cells.

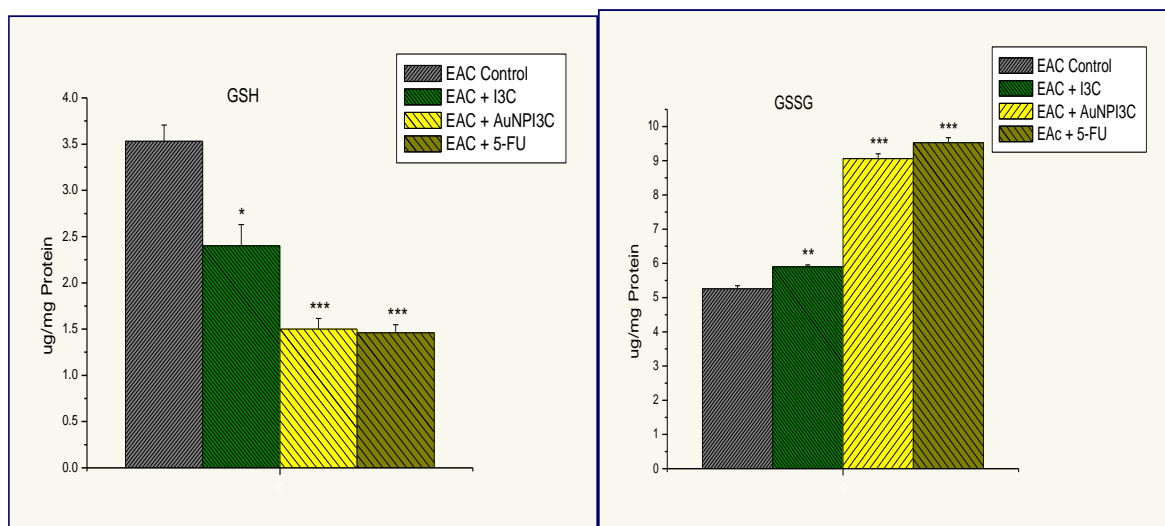


Figure 5.5a: Intracellular reduced glutathione (GSH) levels of EAC cells. 5.5b: Intracellular oxidized glutathione (GSSG) levels of EAC cells. The levels of GSH were expressed as  $\mu\text{g}$  of GSH  $\text{mg}^{-1}$  protein. The levels of GSSG were expressed as  $\mu\text{g}$  of GSSG  $\text{mg}^{-1}$  protein. Cells were treated with AuNPI3Cs and 5-FU for 24 h at  $37^{\circ}\text{C}$ . Values are expressed as Mean $\pm$ SEM of three experiments. ; ‘\*’ indicates a statistically significant difference ( $p < 0.05$ ) ‘\*\*\*’ indicates a statistically significant difference ( $p < 0.001$ ), compared with EAC control group.

### 5.3.4 Effect of AuNPI3Cs on ROS generation in EAC cells

AuNPI3Cs caused increased ROS production as shown by increased DCF fluorescence intensity in the nucleus (Figure 5.6).

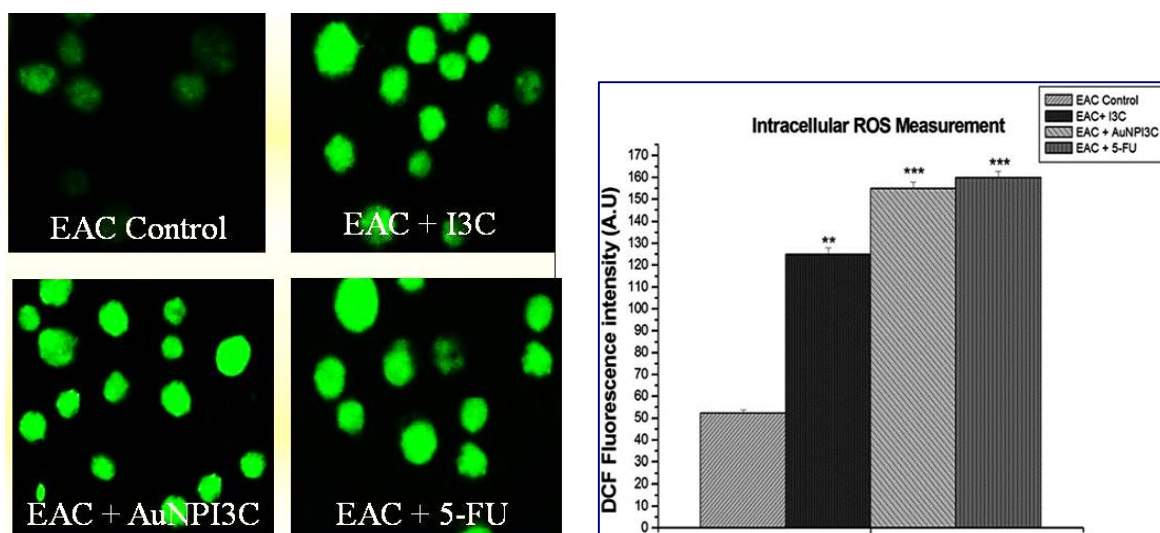


Figure 5.6a: Effects of AuNPI3Cs and 5-FU on reactive oxygen species (ROS) induction in the EAC cell line; Qualitative characterization of ROS formation by H<sub>2</sub>DCFDA staining using fluorescence microscopy. (a) EAC control (b) I3C treated (c) AuNPI3Cs treated (d) 5-FU treated. 5.6b: DCF fluorescence intensity of EAC cells were expressed in graphical form in term of ROS production. Values are expressed as Mean±SEM of three experiments; ‘\*\*’ indicates a statistically significant difference (p<0.001); ‘\*\*\*’ indicates a statistically significant difference (p < 0.001), compared with control.

### 5.3.5 Effect of AuNPI3Cs on cellular morphology in EAC cells

Cell shrinkage and distinct apoptotic blebs were detected in AuNPI3Cs treated EAC (Figure 5.7A) cells. Control cells did not show any alterations but treated cells lost their usual round shape. Scanning electron microscopic observations had shown some morphological and structural changes in EAC cells after AuNPI3Cs treatment (Figure 5.7B).

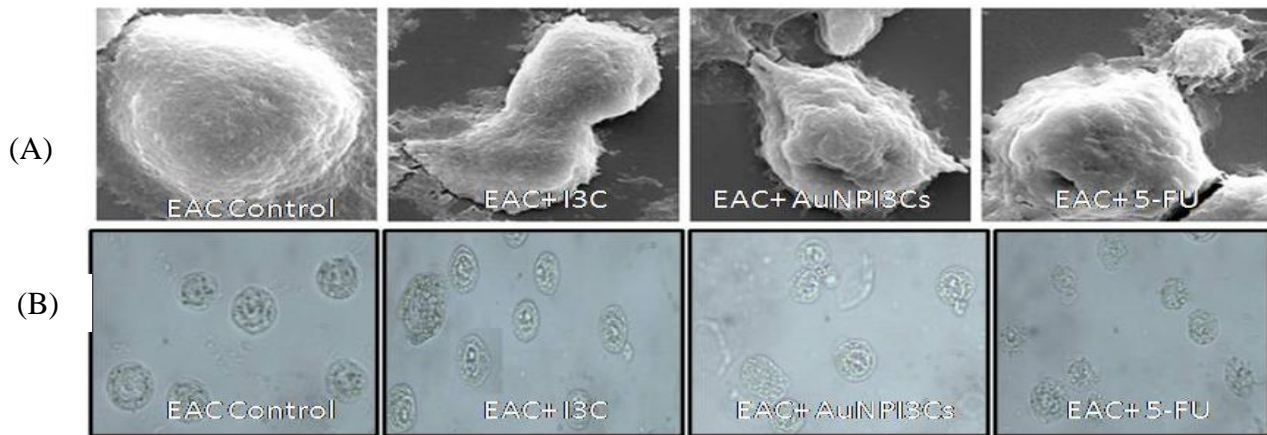


Figure 5.7. (A) Morphological analysis by scanning electron microscopy of EAC cells; (B) Polarizing microscopic analysis of EAC cells. Here, (a) Control EAC cells, (b) I3C treated EAC cells (c) AuNPI3Cs treated EAC cells (d) 5-FU treated EAC cells.

### 5.3.6 Effect of AuNPI3Cs on LDH release in EAC cells

In this study, LDH release was increased after AuNPI3Cs treatment by disrupting the membrane integrity of the EAC cells (Figure 5.8) cells.

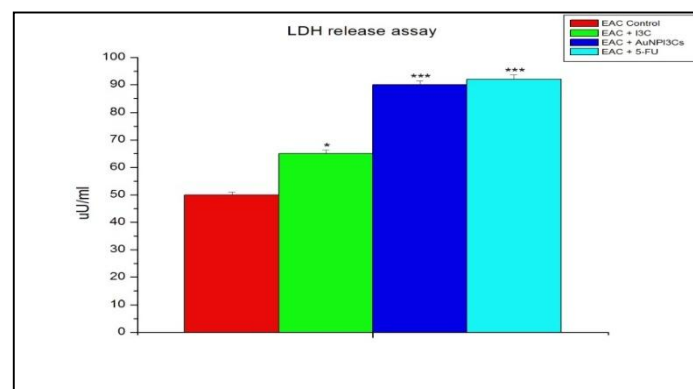


Figure 5.8. Effects of AuNPI3Cs and 5-FU on LDH release assay in EAC cell. Values are expressed as Mean  $\pm$  SEM of three experiments; ‘\*’ indicates a statistically significant difference ( $p < 0.05$ ) ‘\*\*\*’ indicates a statistically significant difference ( $p < 0.001$ ), compared with control group.

### 5.3.7 Effect of AuNPI3Cs on chromatin condensation in EAC cells

In the control group, cells displayed a round shape, and large nuclei were homogenously stained with a less bright red and blue colour. After PI staining, red light emitted from the AuNPI3Cs treated EAC (Figure 5.9A) cells. Cells were much brighter and condensed compared to the control cells. However, the blue light emitted from the treated cells after DAPI staining was much brighter and condensed compared to EAC control (Figure 5.9B) cells.

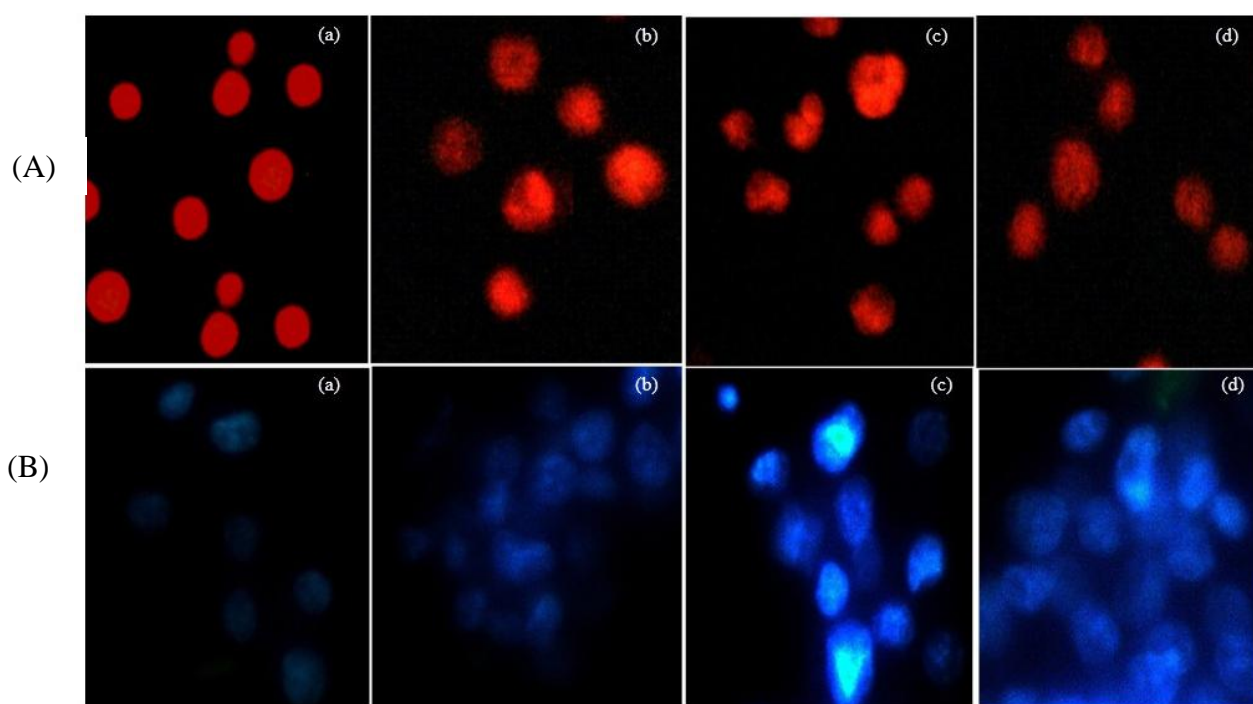


Figure 5.9. Fluorescence- based chromatin condensation study. A. Cells were stained with propidium iodide (PI) B. Cells were stained with DAPI and visualized under a fluorescence microscope to detect chromatin condensation. Here, (a) Control EAC cells, (b) I3C treated EAC cells (c) AuNPI3Cs treated EAC cells (d) 5-FU treated EAC cells.

### 5.3.8 AO-EtBr staining in EAC cells

As shown in Figure 5.10, all the morphological changes were observed in treated EAC cells. Green live EAC cells with a normal morphology were seen in the control group. In contrast,

early apoptotic cells with yellow green dots and late apoptotic cells with orange dots in EAC cell nuclei could be seen in 5-FU treated group and at the same time, green yellow early apoptotic cells were seen in AuNPI3Cs treated group.

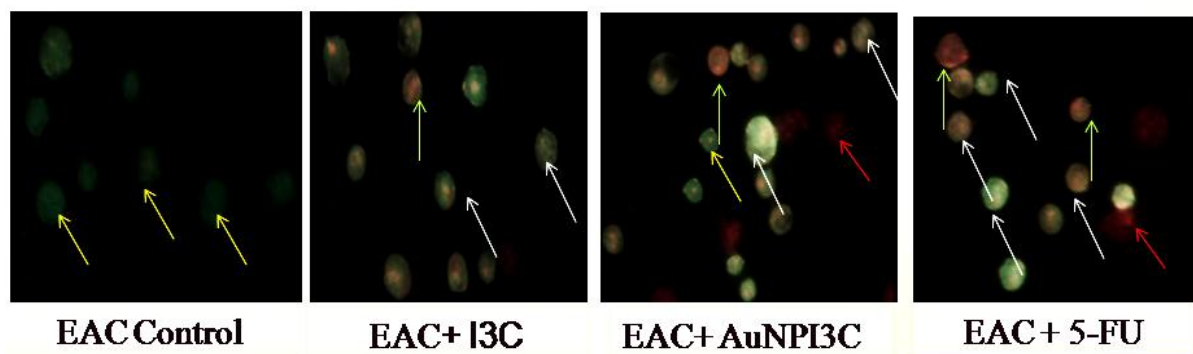


Figure 5.10. EtBr-AO double staining study in EAC cells. Cells were stained with EtBr-AO and visualized under fluorescence microscope. Here, (a) Control EAC cells, (b) I3C treated EAC cells (c) AuNPI3Cs treated EAC cells (d) 5-FU treated EAC cells. White arrow indicates viable cell, yellow arrow indicates early apoptotic cell, blue arrow indicates late apoptotic cell and red arrow indicates necrotic cell.

### 5.3.9 DNA fragmentation study TUNEL assay and alkaline comet assay

DNA content of the cells was estimated by TdT mediated dUTP nick end labeling (TUNEL) assay using flow cytometry (Figure 5.11). As shown in Figure 5.11B we observed that treatment of EAC cells with I3C, AuNPI3Cs and 5-FU resulted in 4.95%, 17.31% and 13.01% TUNEL positive respectively.

From the comet assay it was revealed that AuNPI3Cs treated EAC (Figure 5.12B) cells displayed significant ( $p < 0.001$ ) rise in tail DNA intensity percentage) compared to control. The results were confirmed from fluorescent images (Figure 5.12A).

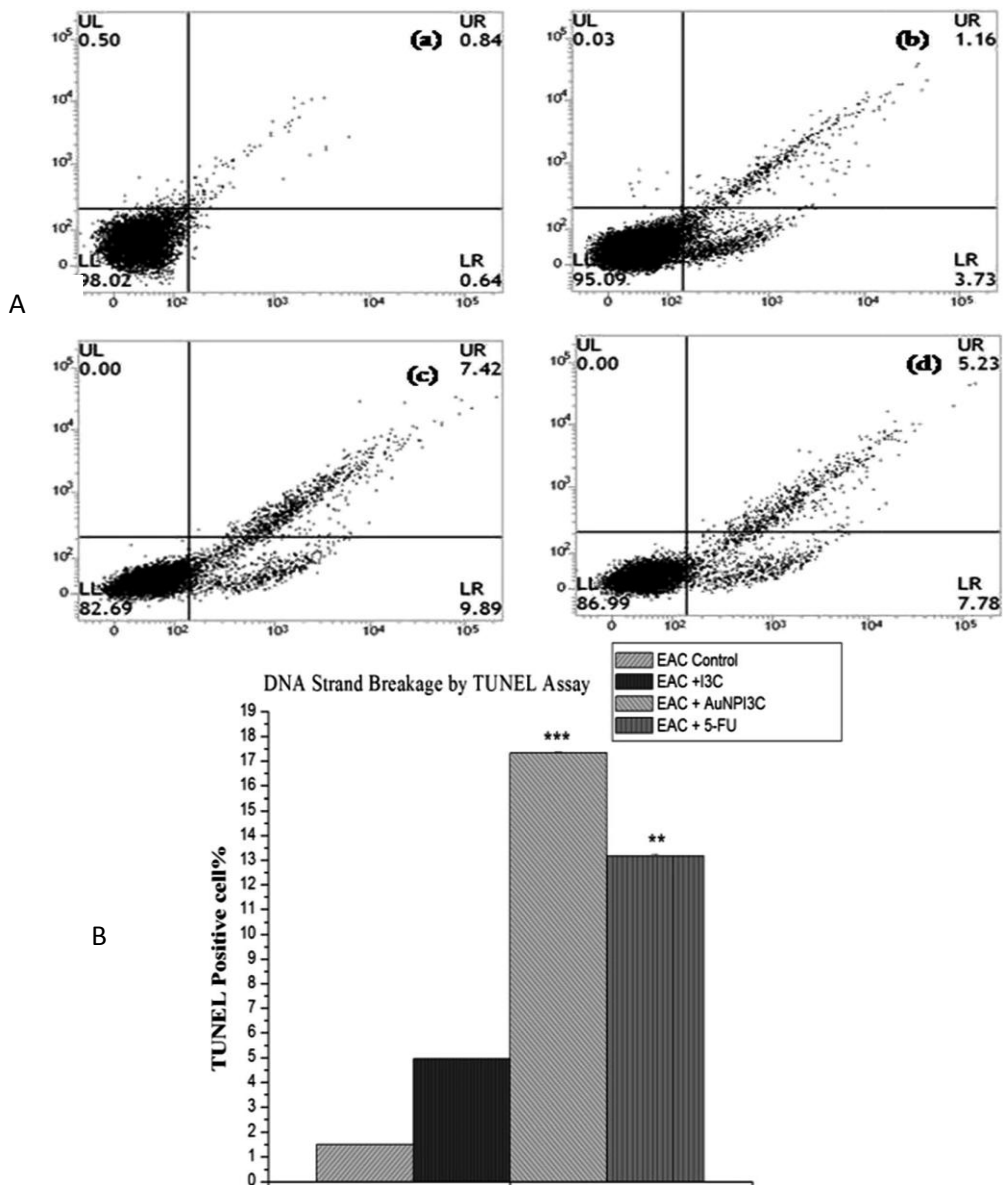


Figure 5.11. AuNPI3Cs-induced apoptosis as measured by TUNEL assay. DNA strand breaks were analyzed by flow cytometry. Here, (a) EAC Control; (b) I3C-treated EAC cells; (c) AuNPI3Cs-treated EAC cells; and (d) 5-FU-treated EAC cells.

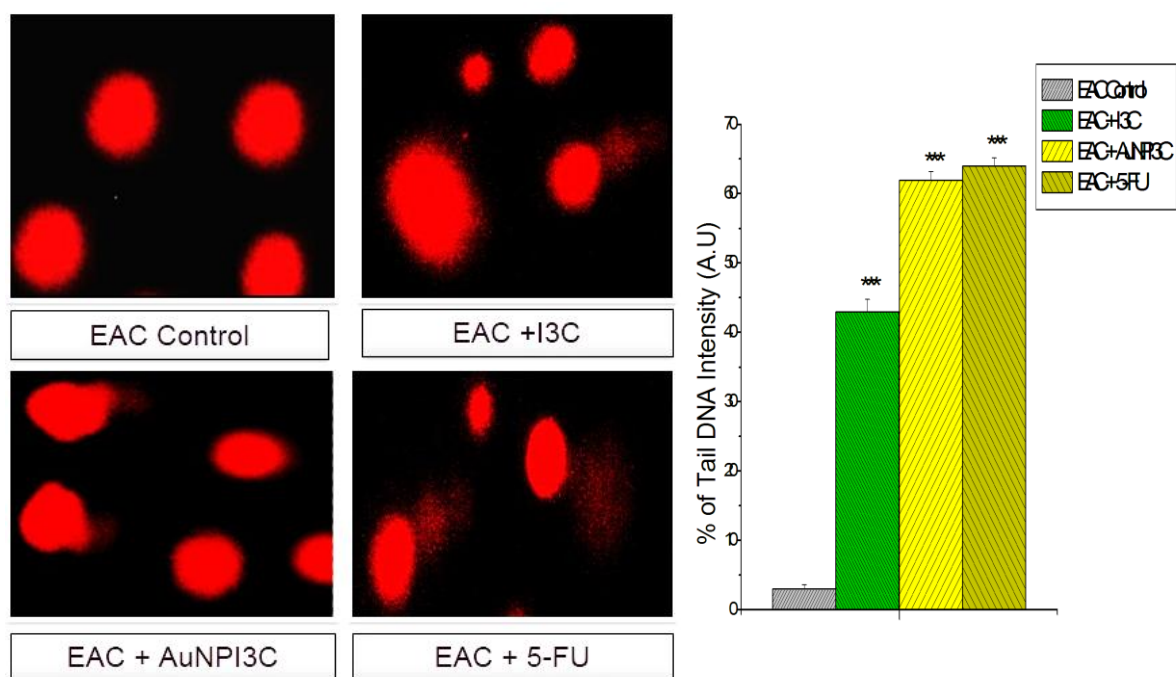


Figure 5.12. Determination of the genotoxic effects of AuNPI3Cs and 5-FU on EAC cells by the Comet assay. (A) Fluorescent microscopic image of (a) EAC control (b) I3C-treated EAC cells, (c) AuNPI3Cs-treated EAC cells, (d) 5-FU treated EAC cells; (B) Estimation of the percentage of tail DNA intensity of AuNPI3Cs and 5-FU on EAC cells. Values are expressed as the mean  $\pm$  SEM of three experiments; '###' indicates a statistically significant difference ( $p < 0.001$ ), compared with the control group.

### 5.3.10 Effect of AuNPI3Cs in Mitochondrial membrane potential ( $\Delta\Psi_m$ )

In this study, it was found that at  $IC_{50}$  dose AuNPI3Cs caused significant depletion of MMP ( $p < 0.001$ ) in the EAC cells compared to control. The mitochondrial membrane potential was estimated based on rhodamine 123 fluorescence intensity. The percentage of MMP decreased significantly ( $p < 0.001$ ) in EAC cells when treated with  $IC_{50}$  dose of AuNPI3Cs.

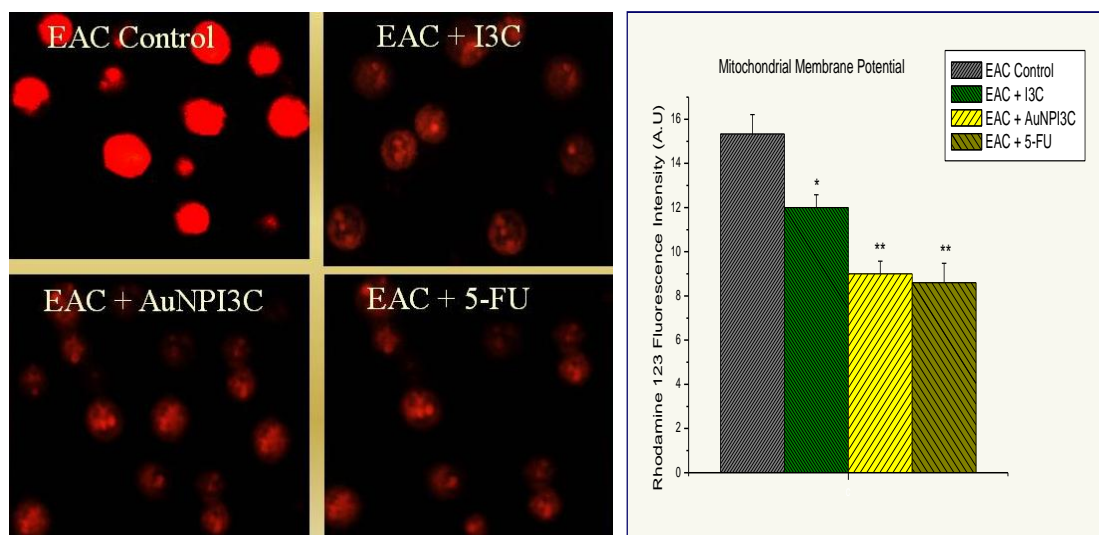


Figure 5.13. A. Measurement of mitochondrial membrane potential (MMP) of AuNPI3Cs and 5-FU treated EAC cells. Values are expressed as Mean $\pm$  SEM of three experiments; ‘\*’ indicates a statistically significant difference ( $p < 0.05$ ), compared with control. ‘\*\*’ indicates a statistically significant difference ( $p < 0.01$ ), compared with control. (a) EAC control (b) I3C-treated EAC cells, (c) AuNPI3Cs-treated EAC cells, (d) 5-FU treated EAC cells. B. Qualitative characterization of mitochondrial membrane potential by Rhodamine 123 staining using fluorescence microscopy. (a) EAC control (b) I3C-treated EAC cells, (c) AuNPI3Cs-treated EAC cells, (d) 5-FU treated EAC cells.

### 5.3.11 Cell Death Analysis-Annexin V-FITC/PI Staining

Flow cytometry analysis of stained cells can distinguish cells into four groups, namely viable (Annexin V-/FITC-PI-), early apoptosis (Annexin V-FITC+ PI-), late apoptosis (Annexin V-FITC+ PI+) and necrotic (Annexin V- FITC-PI+) cells. As shown in Figure 5.14, AuNPI3Cs exposure at  $IC_{50}$  dose resulted in higher population of early apoptotic population (Annexin V-FITC+ PI-), 59.27% in EAC cells compared to EAC control.

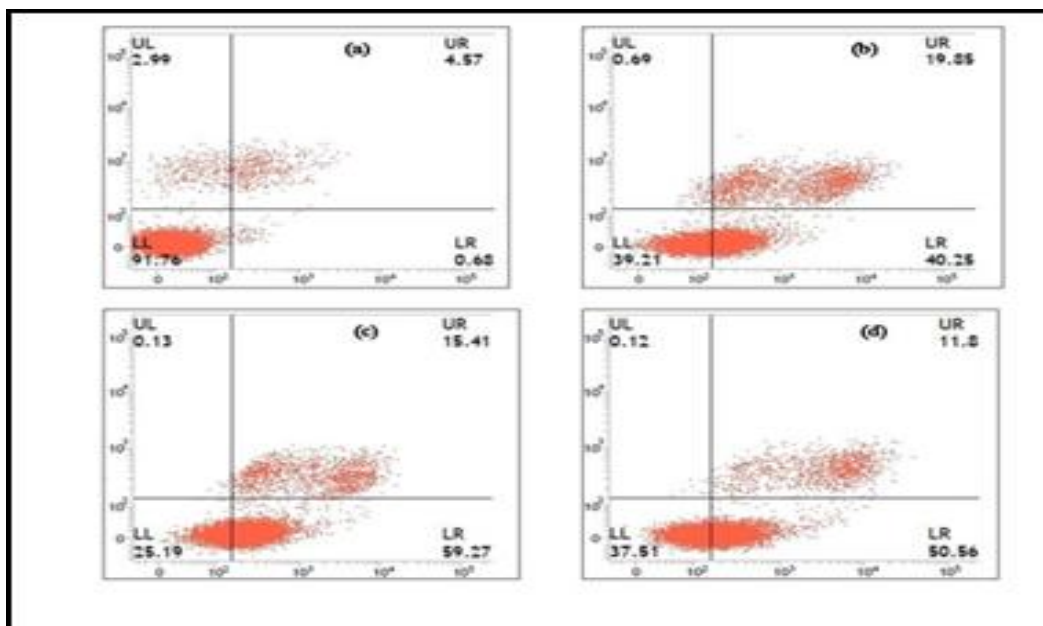


Figure 5.14. FACS analysis of Annexin V-FITC and PI staining of EAC Cells. Cells were treated with AuNPI3Cs and 5-FU for 24 h, stained with Annexin V-FITC and PI and measured by flow cytometry, (a) EAC control (b) I3C-treated EAC cells, (c) AuNPI3Cs-treated EAC cells, (d) 5-FU treated EAC cells.

### 5.3.12 Flow cytometry–based analysis of cellular apoptosis

DNA content of treated EAC cells were analysed by using PI staining, and cell distributions among sub-G1, G0/1, S and G2/M phases were expressed. Cells were treated with the IC<sub>50</sub> concentrations of AuNPI3Cs for 24 h (Figure 5.15). The results revealed that accumulation of G<sub>2</sub>/M phase cells was significantly greater in AuNPI3Cs treated EAC cells than EAC control.

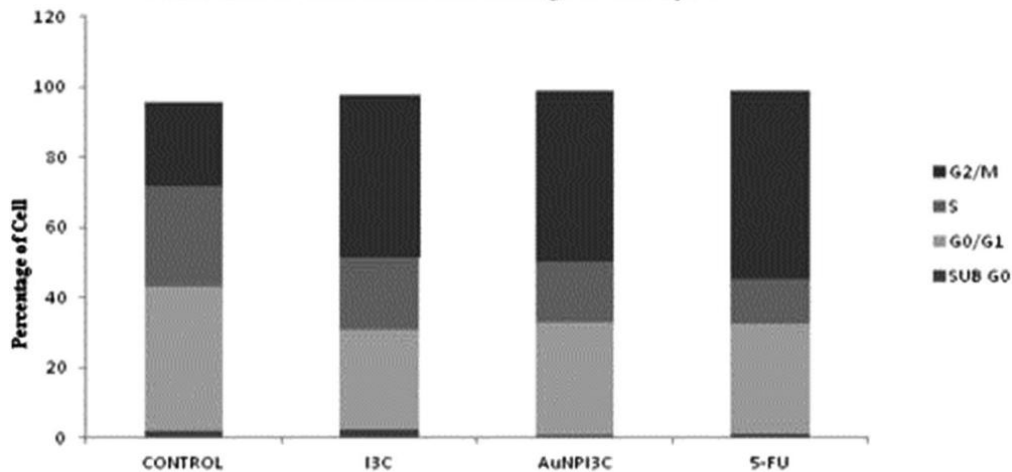
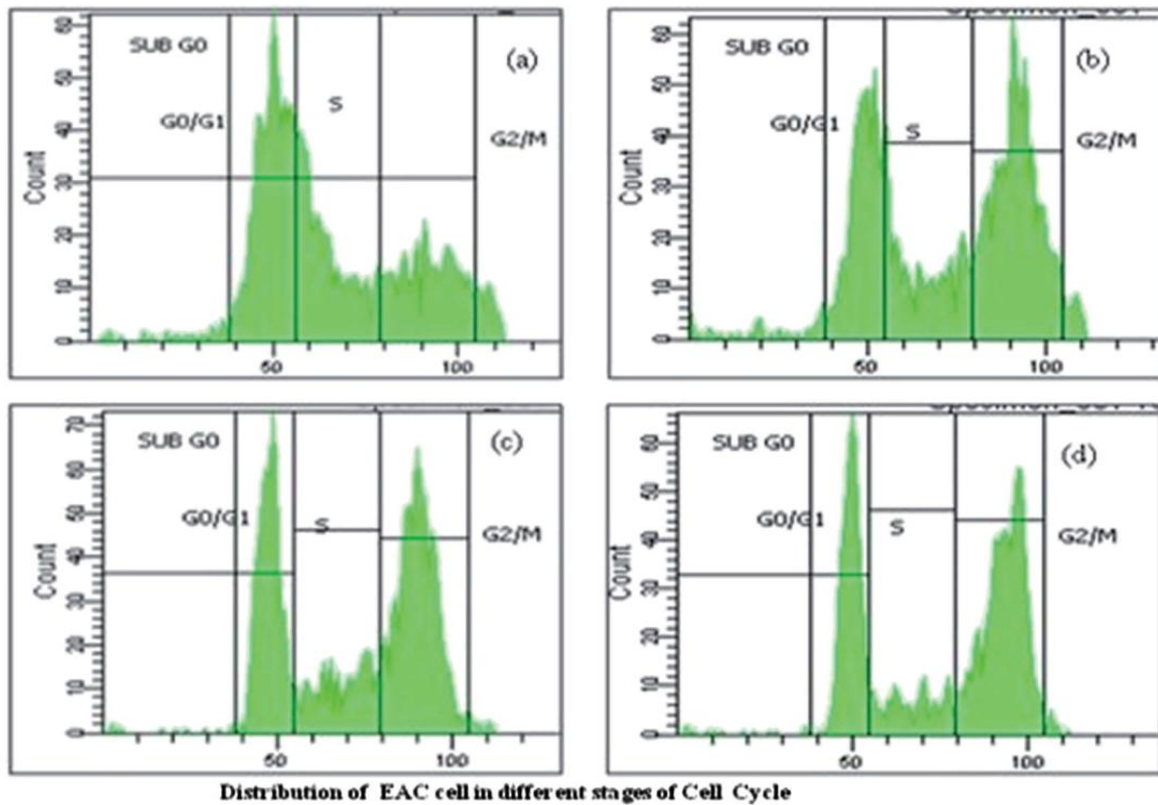


Figure 5.15. Cell cycle arrest analysis by flow cytometry. Cells were treated with AuNPI3Cs and 5-FU for 24 h, stained with PI and measured by flow cytometry (A) Fluorescence activated cell sorting study was done to observe the cell distributions among sub-G<sub>0</sub>, G<sub>0</sub>/G<sub>1</sub>, S and G<sub>2</sub>/M phases in EAC cells. (a) EAC control (b) I3C-treated EAC cells, (c) AuNPI3Cs-treated EAC cells, (d) 5-FU treated EAC cells. (B) Graph shows the percentage of EAC cells in different phases of cell cycle from flow cytometric analysis.

### 5.3.13 Western Blotting

Our data showed that AuNPI3Cs reduced the expression level of Bcl-2 and increased the expression level of Bax, caspase-3 (Figure 5.16).

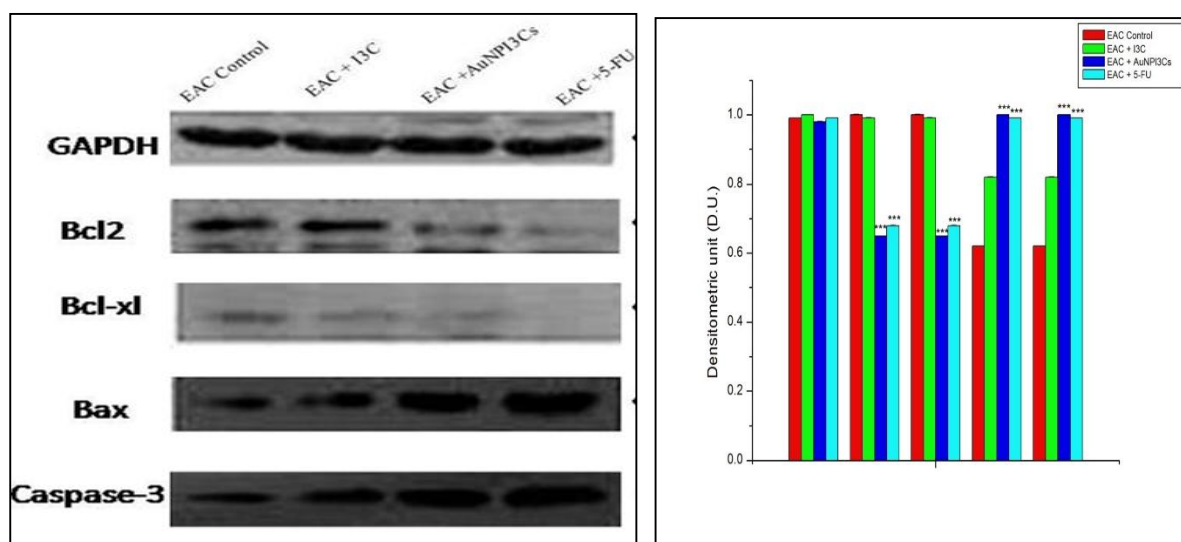


Figure 5.16. Western blot analysis of Bax, Bcl-2 and Caspase-3 proteins in EAC cells treated with AuNPI3Cs and 5-FU for 24 h. Total cell lysates were analyzed by immunoblotting with antibody against anti-Bcl-2, anti-Bax and anti-Caspase 3 antibodies. The results were represented by using Gel-Doc and GAPDH were used as a loading control.

### 5.3.14 Effect of AuNPI3Cs on tumour growth of EAC-bearing mice

#### 5.3.14.1 Effect of AuNPI3Cs in body weight change of tumour bearing mice

Body weight of the mice increases significantly in EAC control group compared to control group, but in I3C and AuNPI3Cs treated groups at doses 1.5/2 mg/kg bwt the body weight was decreased significantly compared to EAC control group (Figure 5.17).

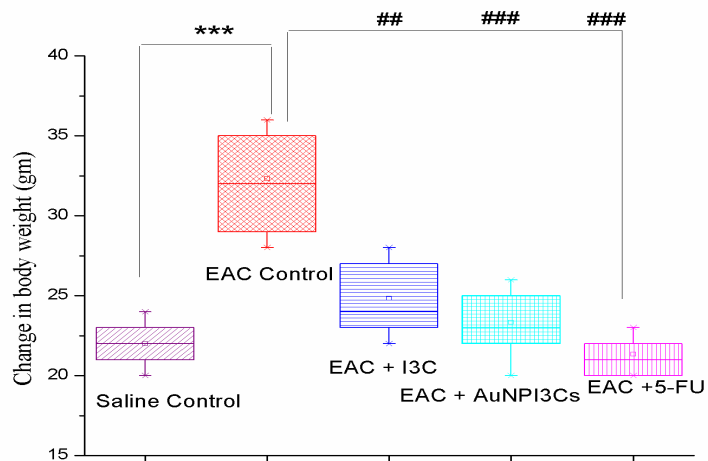


Figure 5.17. The effect of AuNPI3Cs on change of body weight of EAC bearing mice. Data are expressed as Mean $\pm$  SEM.

### 5.3.14.2 Effect of AuNPI3Cs in survival loss, increase life span and mean survival time of tumour bearing mice

Treatment with AuNPI3Cs at the doses of 1.5 and 3 mg/kg bwt increased the mean survival time (MST) (Figure 5.18) by 39.75 $\pm$ 1.1, 36.75 $\pm$ 2.05 days, respectively compared to EAC control group.

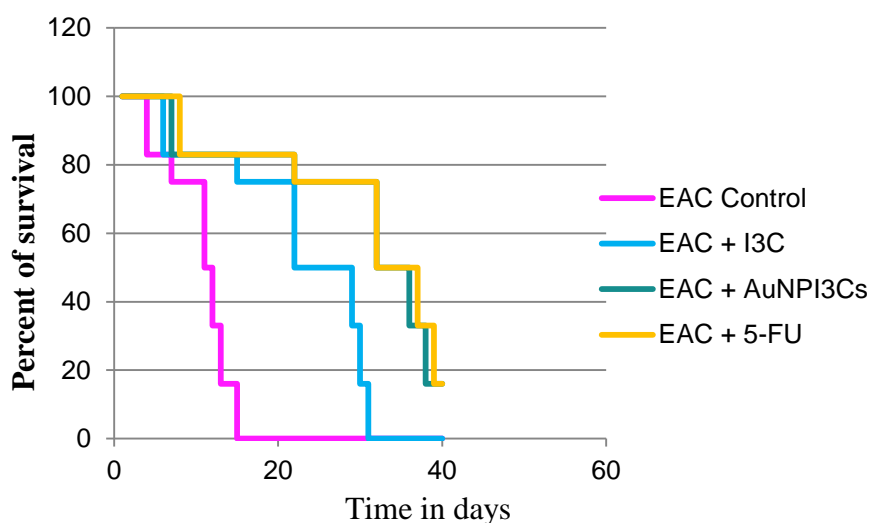


Figure 5.18 The effect of AuNPI3Cs on Mean survival time by Kaplan Meier method in EAC bearing mice. Data are expressed as Mean $\pm$  SEM.

### 5.3.14.3 Effect of AuNPI3Cs in tumour volume in EAC bearing mice

AuNPI3Cs treatment significantly reduced tumour volume (Figure 5.19) compared to tumour control mice.

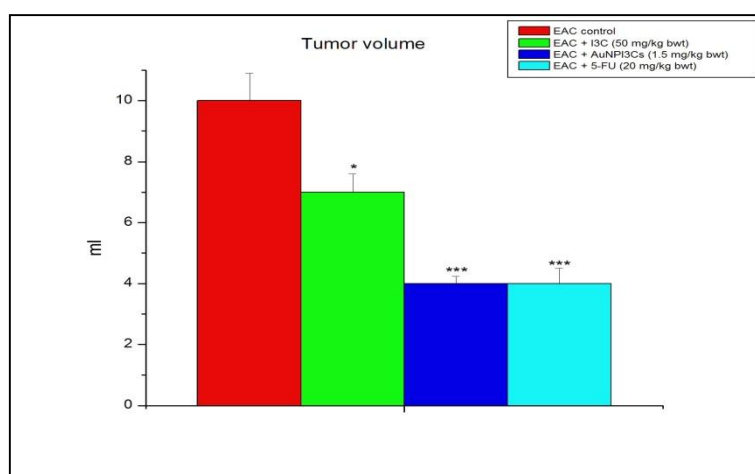
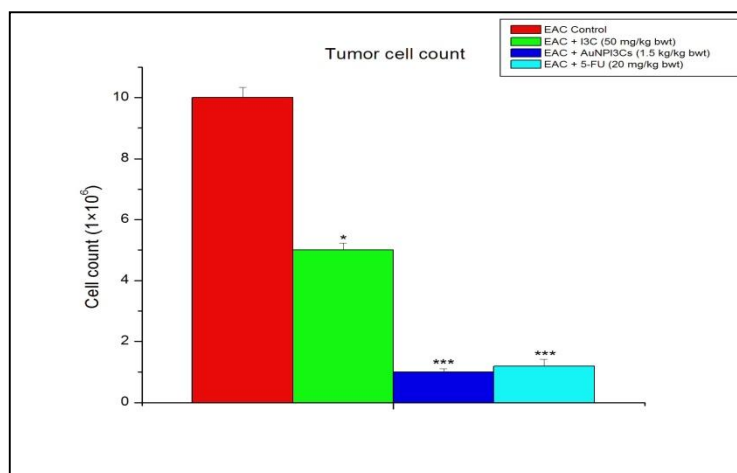


Figure 5.19. The effect of AuNPI3Cs on tumour volume in EAC bearing mice. Data are expressed as Mean  $\pm$  SEM. Probability values are given in asterisks. ‘\*’ indicates significantly difference  $p < 0.05$ ; ‘\*\*\*’ indicates  $p < 0.001$ ; probability values are determined in respect of EAC control.

### 5.3.14.4 Effect of AuNPI3Cs in tumour cell count of tumour bearing mice



**Figure 5.20** The effect of AuNPI3Cs on tumour cell count in EAC bearing mice. Data are expressed as Mean  $\pm$  SEM. ‘\*’ indicates significantly difference  $p < 0.05$ ; ‘\*\*\*’ indicates  $p < 0.001$ ; probability values are determined in respect of EAC and DLA control.

### 5.3.15 Effect of AuNPI3Cs on hematological parameters

The hematological parameters were altered significantly ( $p < 0.001$ ) after 14 days of treatment with AuNPI3Cs when compared to EAC (Table 5.1) control group. It was found that total WBC count was increased significantly in EAC control group whereas, the hemoglobin percentage and RBC count were decreased significantly in the tumor control group. After treating with AuNPI3Cs for 14 days, at doses of 1.5 and 3 mg/kg in case of EAC bearing mice, hematological parameters were brought back towards normal level. These results suggested that AuNPI3Cs have protective role on haemopoietic system. However, the standard drug 5-FU (20 mg/kg body weight) exhibited significant ( $p < 0.001$ ) results in all these haematological parameters

**Table 5.1** Effect of AuNPI3Cs on haematological parameters on EAC bearing mice

Haematological Parameters	Saline Control	EAC Control	EAC + I3C (50 mg/kg bwt)	EAC + I3C (100 mg/kg bwt)	EAC + AuNPI3Cs (1.5 mg/kg bwt)	EAC + AuNPI3Cs (3 mg/kg bwt)	EAC + 5-FU (20 mg/kg bwt)
Hb percentage	12.65±0.17	8.43±0.135 a <sup>***</sup>	10.5±0.15 a*b <sup>*</sup>	11.56±0.13 a* b <sup>**</sup>	12.36±0.117 b <sup>***</sup>	12.7±0.15 b <sup>***</sup>	12.8±0.117 b <sup>***</sup>
Total RBC count (×10 <sup>6</sup> mm <sup>3</sup> )	6.5±0.08	1.76±0.08 a <sup>***</sup>	5.6±0.06 a* b <sup>***</sup>	5.9±0.05 a*b <sup>***</sup>	6±0.02 b <sup>***</sup>	6.2±0.002 b <sup>***</sup>	5.9±0.017 a* b <sup>***</sup>
Total WBC count (/μl)	4100±32	8900±102 a <sup>***</sup>	6000±52 a*b <sup>**</sup>	5500±40 a*b <sup>***</sup>	5400±55 a*b <sup>***</sup>	4900±24 b <sup>***</sup>	4800±28 b <sup>***</sup>

Data are expressed as Mean± SEM (n=6). a<sup>\*\*\*</sup> represents significant difference at (p<0.001) compared to saline control; ‘b<sup>\*\*</sup>’ represents significant difference at (p<0.01); ‘b<sup>\*\*\*</sup>’ represents significant difference at (p<0.001) compared to EAC control.

### 5.3.16 Effect of AuNPI3Cs on antioxidant parameters

The level of lipid peroxidation in liver and kidney tissue was significantly increased in tumor control mice when compared to saline control mice. After administration of AuNPI3Cs (1.5 and 3 mg/kg bwt) in case of EAC bearing mice, lipid peroxidation levels were significantly decreased when compared with tumour control mice. Similarly, reduced glutathione level (GSH) were changed in tumour control compared to saline control, restored to the near normal values after treatment with AuNPI3Cs as well as 5-FU. In tumour control mice there were significant reduction in antioxidant enzymes like super oxide dismutase (SOD), catalase which were significantly improved by the treatment of AuNPI3Cs as well as 5-FU. GPx and GST levels both were decreased significantly in tumour control group, AuNPI3Cs treatment increased significantly.

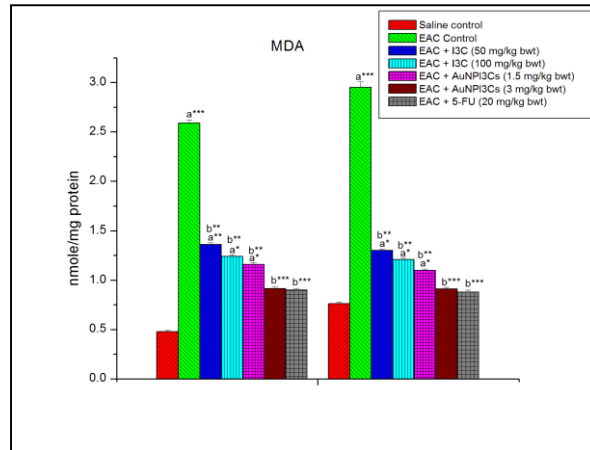


Figure 5.21 shows the effect of AuNPI3Cs on liver and kidney MDA after 15 days treatment in EAC bearing mice. Data are expressed as Mean± SEM (n=6). a\*\*\*'represents significant difference at (p<0.001) compared to saline control; 'b\*\*' represents significant difference at (p<0.01); 'b\*\*\*\*' represents significant difference at (p<0.001) compared to EAC control.

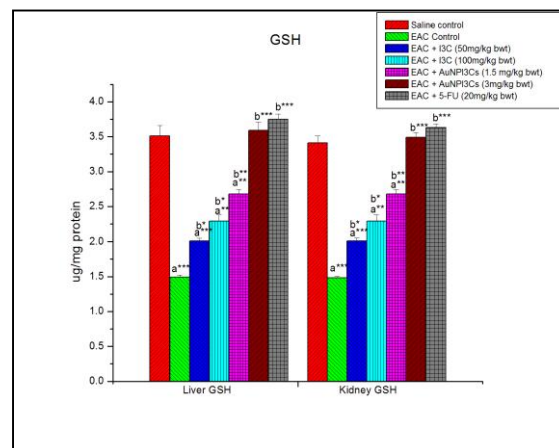


Figure 5.22 shows the effect of AuNPI3s on liver and kidney GSH after 15 days treatment in EAC bearing mice. Data are expressed as Mean± SEM (n=6). a\*\*\*'represents significant difference at (p<0.001) compared to saline control; 'b\*\*' represents significant difference at (p<0.01); 'b\*\*\*\*' represents significant difference at (p<0.001) compared to EAC control.

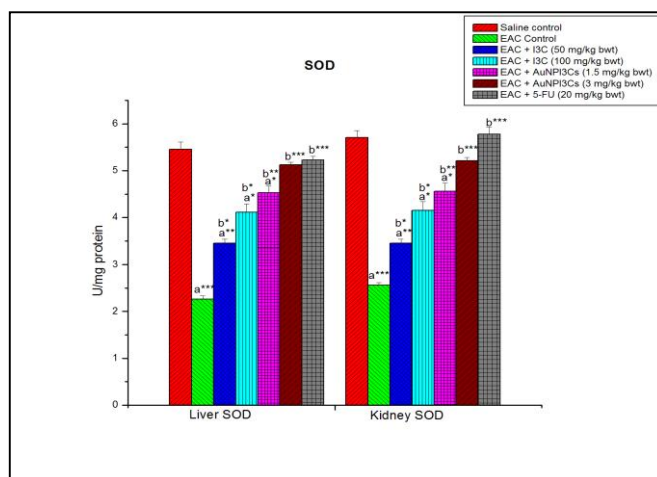


Figure 5.23 shows the effect of AuNPI3Cs on liver and kidney SOD after 15 days treatment in EAC bearing mice. Data are expressed as Mean $\pm$  SEM (n=6). 'a\*\*\*' represents significant difference at (p<0.001) compared to saline control; 'b\*\*' represents significant difference at (p<0.01); 'b\*\*\*' represents significant difference at (p<0.001) compared to EAC control.

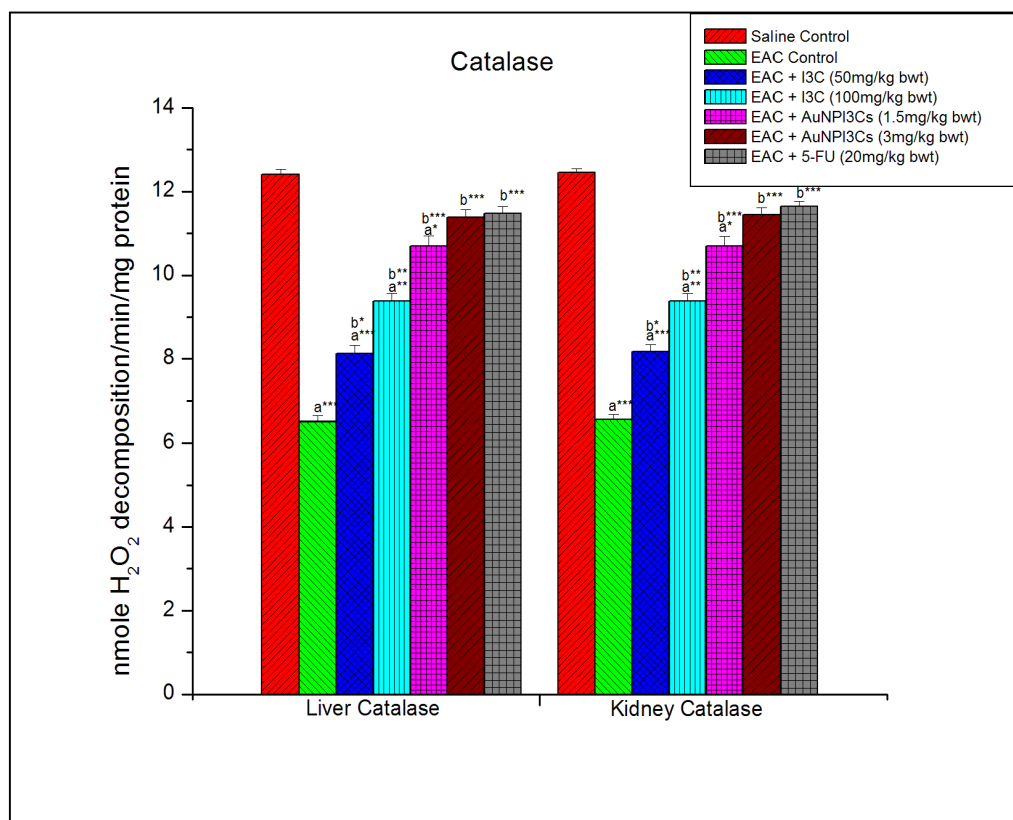


Figure 5.24 shows the effect of AuNPI3Cs on liver and kidney Catalase after 15 days treatment in EAC bearing mice. Data are expressed as Mean± SEM (n=6). a\*\*\*'represents significant difference at (p<0.001) compared to saline control; 'b\*\*' represents significant difference at (p<0.01); 'b\*\*\*' represents significant difference at (p<0.001) compared to EAC control.

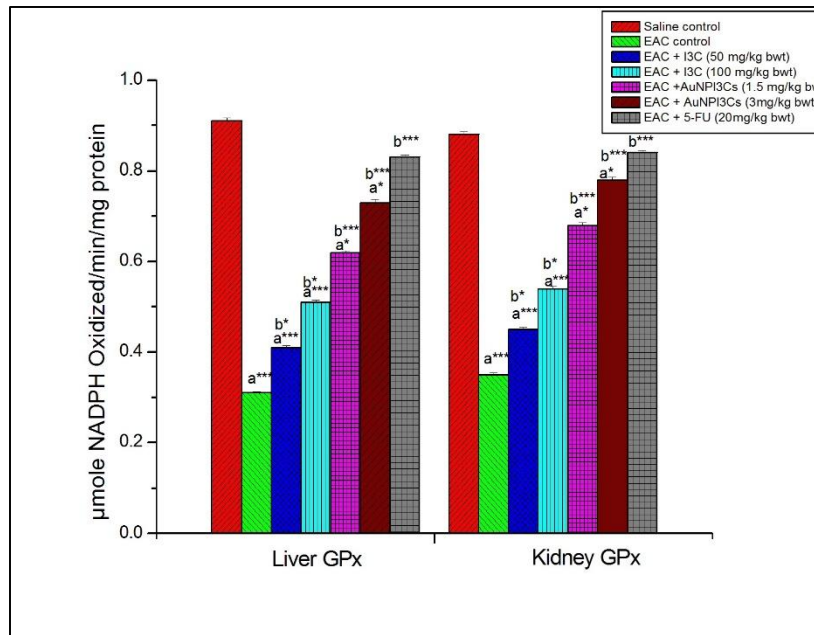


Figure 5.25 shows the effect of AuNPI3Cs on liver and kidney GPx after 15 days treatment in EAC (bearing mice. Data are expressed as Mean± SEM (n=6).

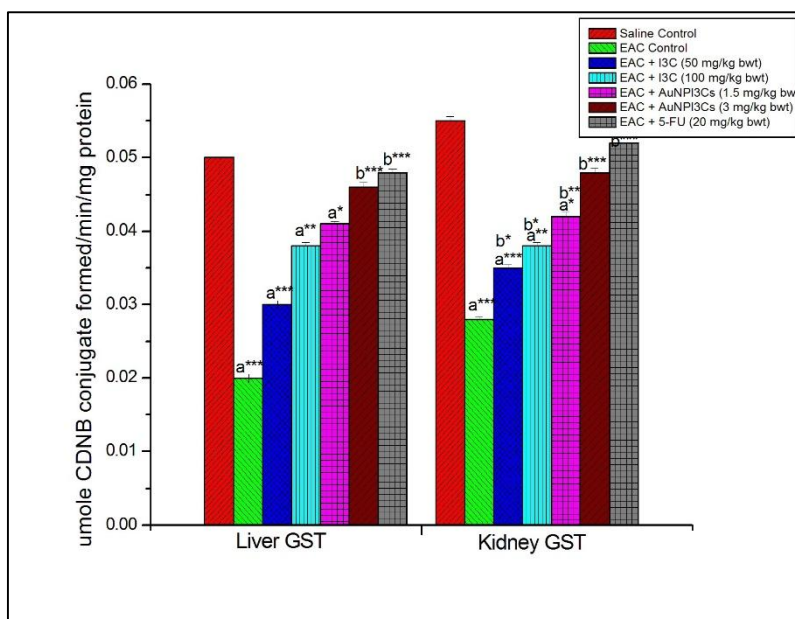


Figure 5.26 shows the effect of AuNPI3Cs on liver and kidney GST after 15 days treatment in EAC bearing mice. Data are expressed as Mean± SEM (n=6).

### 5.3.17 Tumour growth in EAC–induced solid tumor

The effect of AuNPI3Cs on EAC induced solid tumors in Swiss albino mice was performed, and the results are presented in figure 5.27, 5.28. AuNPI3Cs treatment significantly reduced tumor size and tumor mass ( $p < 0.001$ ) compared to control (Figure 5.27B). Reduction in tumor volume after treatment with AuNPI3Cs is shown in figure 5.27C. Immunohistochemical staining of tumor masses sections exhibited decreased expression of CD31 in AuNPI3Cs treated tumors. Immunohistochemical analysis of Ki-67 confirmed the antiproliferative functions of AuNPI3Cs (Figure 5.28).

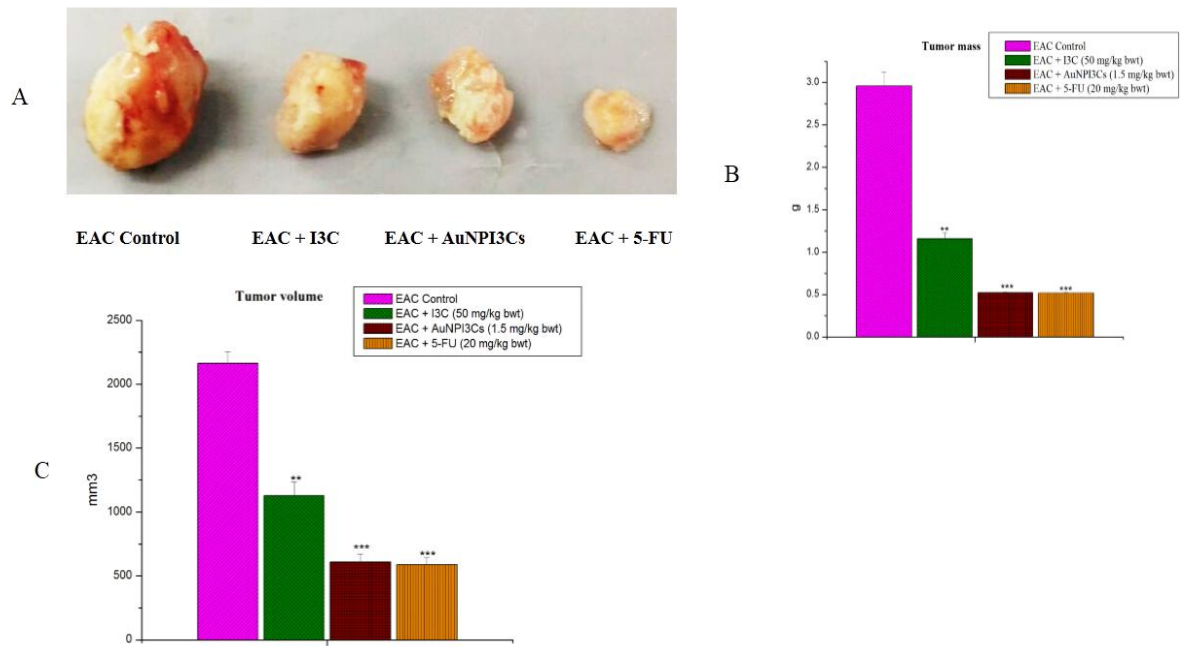


Figure 5.27 A: Solid tumour regression study in EAC induced mice after subcutaneous injection of I3C (50 mg/kg/day) and AuNPI3Cs (1.5 mg/kg/day) for 28 days. B: Bar graph represents tumour masses in gram in EAC induced mice. C: Tumour volume in EAC induced mice after subcutaneous injections of I3C and AuNPI3Cs. Data represents as Mean  $\pm$ SEM; (\*\*indicates  $p < 0.01$  and \*\*\*represents  $p < 0.001$ ).

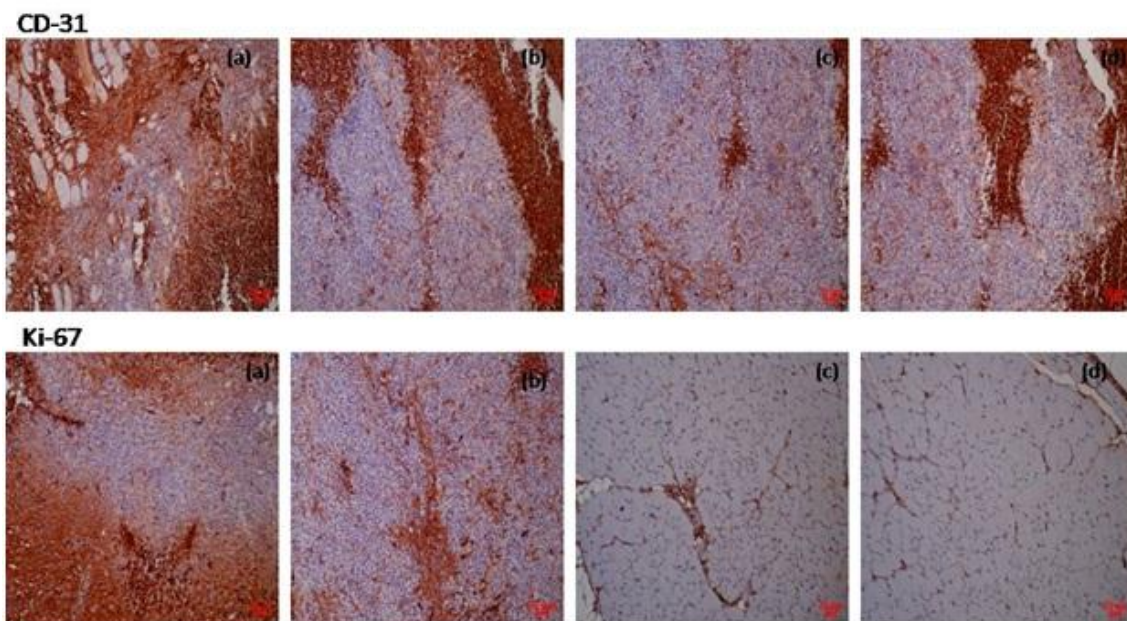


Figure 5.28 Immuno-histochemical CD-31, Ki-67 expression in EAC-induced solid tumour from mice treated with subcutaneous injection of I3C (50 mg/kg/day) and AuNPI3Cs (1.5 mg/kg/day) for 28 days. Paraffin-embedded sections of tumours are processed and immuno-histochemical assays of CD-31, Ki-67 are performed.

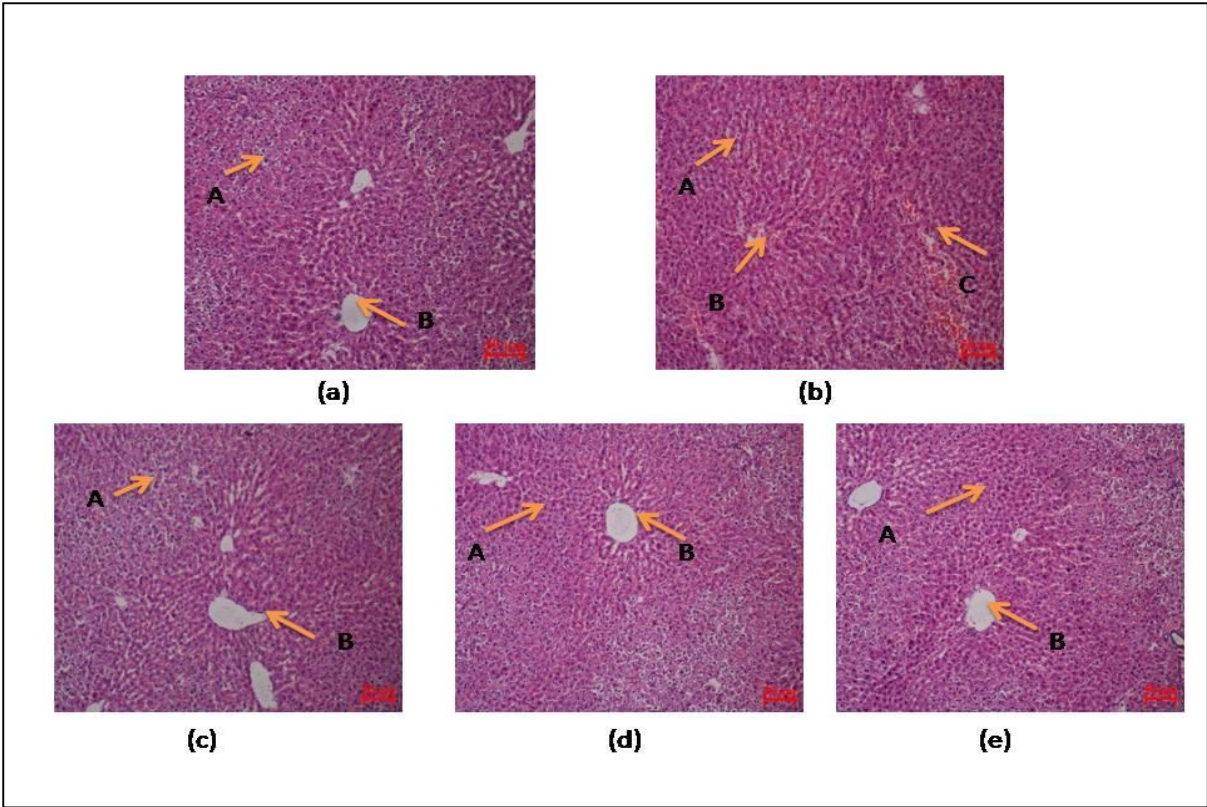


Figure 5.29 Histological alterations of liver after treatment of AuNPI3Cs in EAC bearing Swiss albino mice. (scale bar = 50  $\mu$ m)

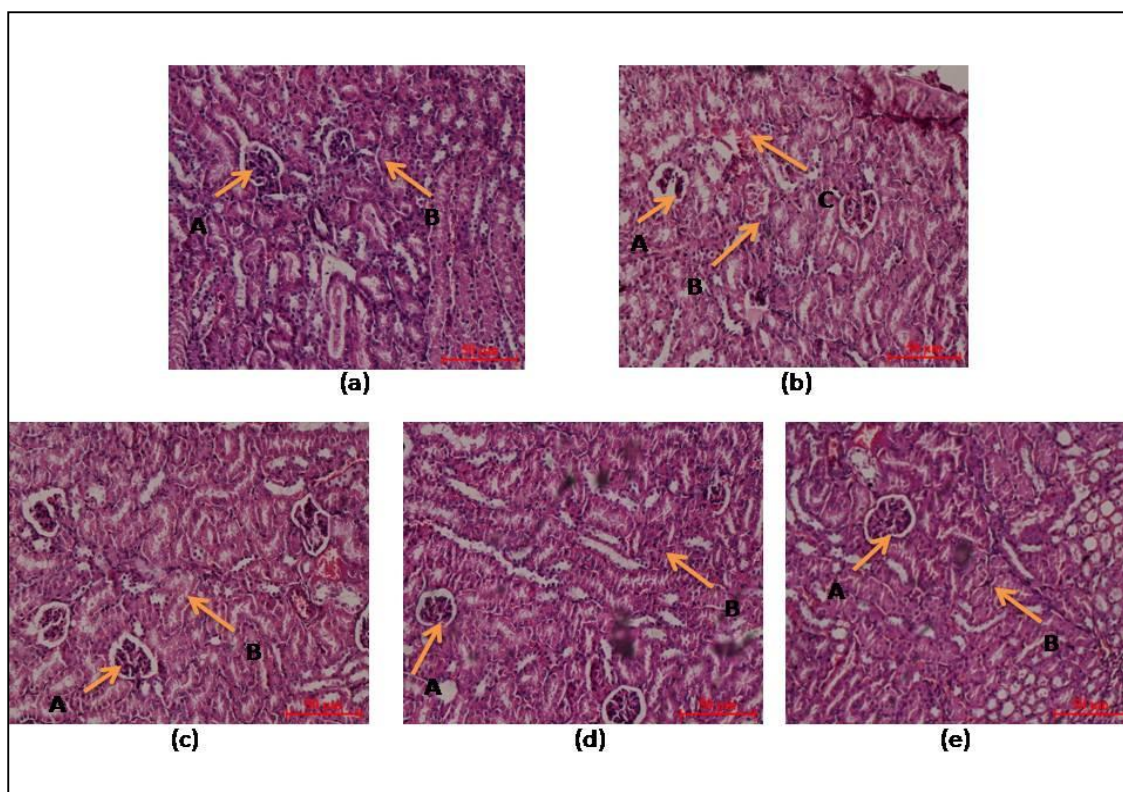


Figure 5.30 Histological alterations of kidney after treatment of AuNPI3Cs in EAC bearing Swiss albino mice. (scale bar = 50  $\mu\text{m}$ )

#### 5.4 Discussion

The dose dependent cytotoxicity was observed in AuNPI3Cs treated EAC cells. Earlier studies have pointed out that nanoparticles persuade cytotoxicity via the formation of reactive oxygen species or upsurges cellular oxidative stress and activate cell death process including apoptosis and necrosis (Sumana et al., 2013). At  $\text{IC}_{50}$  value ( $5\mu\text{g ml}^{-1}$ ) of AuNPI3Cs, no trace of cytotoxicity was observed in human lymphocytes. These data created interest as it suggested that AuNPI3Cs were more toxic to cancer cells compared to normal cells.

In this study, active internalization of Rhodamine-B tagged AuNPI3Cs were seen in EAC cells by fluorescence microscopy and the fluorescence intensity was estimated by AAS. It

was observed that rhodamine-B tagged AuNPI3Cs were well distributed throughout the EAC cells. AAS study confirmed that the drug uptake in EAC cells was significantly increased compared to normal lymphocytes. The internalization processes of nanoparticles may be occurred by phagocytosis, pinocytosis or endocytosis and are dependent on particle size and cell type used (Gyenge et al., 2011).

Cellular GSH content is diminished due to the oxidation of GSH to glutathione disulphide (GSSG) in many pathological conditions. GSH/GSSG ratio is decreased in oxidative stress (Gr̃avil̃a et al., 2010).

The present study exhibited the decreased GSH (Figure 5.4A) and increased GSSH (Figure 5.4B) levels in AuNPI3Cs treated EAC cells. So, by altering the intracellular redox status, AuNPI3Cs may decrease EAC cell viability.

Reactive oxygen species (ROS) generation has an important role in apoptosis mediated cancer cell death (MateÂs and SaÂnchez-JimeÂnez, 2000). ROS are exceptionally active and play a vital role in cell signalling, leading to oxidative cell injury due to unpaired valence shell electrons (Thannickal and Fanburg,2000). Intracellular ROS generation occurs from mitochondrial respiratory chain reaction and membrane-bound superoxide-generating enzyme i.e., nicotinamide adenine dinucleotide phosphate (NADPH) oxidase mediated reactions. Furthermore, reduction of oxygen may either yield H<sub>2</sub>O<sub>2</sub> or OH<sup>-</sup> via SOD catalysed reaction and metal-catalyzed Fenton-like reactions, respectively (Pereira et al, 2012). After exposure to AuNPI3Cs for 24 h, EAC cells showed (Figure 5.6) enhanced ROS formation as shown by the increased DCF fluorescence intensity.

Cell shrinkage and distinct apoptotic blebs were detected in AuNPI3Cs treated EAC cells. Control cells did not show any alterations but the treated cells lost their usual round shape (Figure 5.7). This may be due to apoptotic cascade and caspase-facilitated events indicated by

distinctive apoptotic morphologies which include shrinkage of cellular volume, chromatin condensation (pyknosis) and segregation along the nuclear membrane. Chromosomal DNA cleavage into internucleosomal fragments, phosphatidylserine externalization and intracellular substrate cleavage by specific proteolysis also occurs (Martin and Green, 1995). Scanning electron microscopic observations had occurred some morphological and structural changes in EAC cells after AuNPI3Cs treatment. AuNPI3Cs treated EAC cells displayed some cytoplasmic extrusion and echinoid spikes (Figure 5.7B) as well as reduced cell-cell contacts. Membrane blebbing and cell shrinkage were also found in SEM analysis.

LDH is a cytoplasmic enzyme released into extracellular space when cell membrane (Saad et al.,2006). In this study, AuNPI3Cs were found to upsurge LDH release by disrupting the membrane integrity of EAC cells (Figure 5.7). The intracellular LDH release to the medium is an indication of irreversible cell death caused by cell membrane damage and also it is reported (Xia et al.,2007) that LDH upregulation directly induce apoptosis.

Chromatin condensation is a typical characteristic of apoptosis (Hacker,2000). The red-fluorescent propidium iodide is a DNA-binding dye, which can stain the cells during increased plasma membrane permeability and loss of plasma membrane integrity. The blue fluorescent dye DAPI generally used to stain the condensed nuclei of apoptotic cells. After staining with PI and DAPI it had been revealed that AuNPI3Cs induced several features of apoptosis such as condensed chromatin and fragmented punctuate red and blue nuclear fluorescence in EAC cells (Figure 5.8 and 5.9). As membrane integrity became compromised; PI and DAPI stain leaked into intact membrane, even in shrunken cell, the apoptotic nuclei appeared bright pink chromatin and bright blue chromatin that are highly condensed and fragmented (Bortner and Cidlowski, 1998).

The cells which have intact DNA and nuclei have a round and green nucleus is recognized as viable cells. Early apoptotic cells possess appeared with yellowish green coloured nuclei. Late apoptotic and necrotic cells were stained orange and red respectively. From Figure 5.10, it is clearly evident that AuNPI3Cs caused cell death through apoptosis. Because most of the AuNPI3Cs treated cells showed features of late apoptotic and minimum number of cells necrosis (Suman et al.,2012).

The ability of AuNPI3Cs to induce apoptosis is also supported by measuring the DNA damage in cells. As shown in Figure 5.11, TUNEL-positive cells were detected by flow cytometry which indicates apoptotic cells with the presence of DNA fragments. During apoptosis, DNA strand breaks expose the 3'OH ends which act as sites for the addition of fluorescein dUTP. The incorporation was detected using fluorescein-dUTP to label DNA strand breaks (Darzynkiewicz et al., 2008).

From the comet assay it was revealed that AuNPI3Cs caused significant rise in tail DNA intensity percentage in EAC cells compared to EAC control.

Tail DNA percentage can be increased by the direct induction of DNA strand breaks or disruption of DNA backbones by nanoparticles or it's by products (Dash et al., 2014). This nanoparticles-induced genotoxicity has no clearly understood mechanism. After crossing the nuclear membrane nanoparticles directly or indirectly interact with DNA (Asare et al., 2012). Rhodamine 123 fluorescence study measures mitochondrial membrane potential (MMP). AuNPI3Cs treatment decreased of MMP in EAC cell suggested a possible disturbance of the cellular mitochondrial membrane. AuNPI3Cs-treated cells showed an alteration in  $\Delta\Psi_m$  and it may be due to malfunction in ATP synthesis and maintenance of the ATP level that leads to either apoptosis or necrosis. A lowered level of ATP activates apoptosis induced cell death (Adrie et al., 2001).

One of the events, cells which are undergoing apoptosis exposed phosphatidylserine from the inner side of the plasma membrane to its outer leaflet. Cells can bind to Annexin V and this process can be used as a marker of apoptosis (Bhatia et al.,2015). After 24-h exposure to AuNPI3Cs, the number of early apoptotic cells (Annexin V and PI positive)increased compared to control. Although both late apoptotic and necrotic cells are Annexin V and PI positive, the presence of these cells with early apoptotic cells suggests that such dead cells resulted from the apoptosis rather than necrosis (George et al.,2015).These findings confirmed that apoptosis may be the possible mechanism by which AuNPI3Cs triggers cell death in EAC cells (Figure 5.16).

Cell cycle arrest due to DNA damage can activate cell death via apoptosis. DNA content of treated EAC cells was analysed by using PI staining, and cell distributions among sub-G1, G0/1, S and G2/M phases were expressed. Results revealed increasing accumulation of cells at the G<sub>2</sub>/M phase. Accumulation of G<sub>2</sub>/M phase cells was significantly greater in cells treated with AuNPI3Cs than in controls validating the results of the MTT cell proliferation assay. DNA damage may extrude cyclin B1 from the nucleus which promote G<sub>2</sub>/M phase arrest (Drews-Elger et al.,2009).Cells have mechanisms to continue genomic stability through cell cycle arrest (Xue et al.,2012). It is evident that alteration in cell cycle checkpoints cause cell cycle arrest which leads to apoptosis (Davis et al.,2009). AuNPI3Cs may take part in up or down regulation of G<sub>2</sub>/M checkpoint proteins which leads to cell cycle arrest.

Apoptosis is regulated by Bcl-2 and Bax ratio and proteins of the Bcl-2 family show a typical role in caspase activity. From the present study it has been shown that after AuNPI3Cs treatment, Bcl-2 protein was down regulated and Bax was up regulated (i.e.,increased Bax/Bcl-2 ratio) in EAC cells (Figure 5.18). Through activation of mitochondrial cytochrome C release, higher Bax/Bcl-2 ratio generates apoptotic signaling (Das et al., 2012). From these

results, it is suggested that AuNPI3Cs induced apoptotic death in EAC cells by the intrinsic mitochondrial pathway (Elmore, 2007).

The body weight of AuNPI3Cs treated mice was decreased compared to control EAC bearing mice. Tumour volume and tumour cell count also decreased in AuNPI3Cs-treated tumour bearing mice. This reduction could be positively correlated with the ascites fluid volume or tumour volume. Ascites fluid provides the nutritional source for tumour cells (Prasad and Giri, 1994). Prolongation of life span is a reliable criterion to evaluate an anticancer drug (Rajesh et al., 2011). With reliability to this, average life span of AuNPI3Cs treated mice increased considerably. Reduction in body weight and ascites fluid volume as well as prolongation of lifespan indicates the restorative prognosis of cancer (Hogland, 1982).

Immunohistochemical staining of tumour tissues displayed reduced expression of Ki-67 in AuNPI3Cs-treated tumours, suggesting the antiproliferative effects of biogenic AuNPI3Cs. Immunohistochemical analysis of CD-31 established the anti-angiogenic action of AuNPI3Cs. Hematological parameters were significantly restored towards normal ranges in EAC induced group after treatment of AuNPI3Cs.

Tumour growth can cause antioxidant disturbances in tissues (Badr, 2004). Malondialdehyde (MDA) is an end product of oxidative degeneration has been reported to be higher in cancer tissues (Valenzuela, 1991). The levels of MDA were found to be rapidly increased in tumor induced animals and returned back near to normal after treatment of AuNPI3Cs. Intracellular protection against free radicals, peroxide and toxic compounds is provided by glutathione. Tumour development noticeably decreased cellular GSH, which may occur due to oxidative stress (Grăvilă et al., 2010). Increased free radicals in tumour cells causes reduced levels of GSH for the effective conversion of GSH to GSSG. Significant increment in liver and kidney GSH was attained by the treatment of AuNPI3Cs and I3C, representing the protecting role of

AuNPI3Cs and I3C in EAC bearing mice. The levels of catalase (CAT), superoxide dismutase (SOD) were decreased in EAC bearing mice and increased significantly near to normal after treatment with AuNPI3Cs.

GPx, in saline control mice was increased compared to tumour control group mice but this level was brought to near-normal after the treatment of AuNPI3Cs. Administration of AuNPI3Cs resulted in restoration of antioxidant properties equivalent to that of 5-FU, the standard drug. Altogether, it is evident that AuNPI3Cs protect the host tissues from oxidative stress by restoring the antioxidant enzyme system. Histopathological studies also showed the level of damage to liver cells in EAC bearing mice. Histopathological studies also revealed the recovery of liver architecture after treatment of AuNPI3Cs in EAC bearing mice. In this study, tumour induced mice treated with AuNPI3Cs showed that kidney histoarchitecture was almost similar to that of normal group. From this observation it could be understood that AuNPI3Cs induce apoptosis in tumour cells without affecting the normal cells.

## **5.5. Conclusion**

AuNPI3Cs produced cytotoxicity on Ehrlich ascites carcinoma (EAC) cells showing IC<sub>50</sub> value of 5 µg ml<sup>-1</sup> respectively and showed non-toxic nature to mice lymphocytes up to the level of 25 µg ml<sup>-1</sup>. The cytotoxic effect of AuNPI3Cs was correlated with elevation of ROS, decrease in mitochondrial membrane potential, DNA fragmentation, cell cycle arrest, imbalance of apoptotic proteins. The antitumor activity noticed in mice model strongly may be due to the hemoprotective, hepatoprotective and antioxidant properties of AuNPI3Cs.